Geological Characterization of the Patterson CO_2 Storage Site from 3-D Seismic Data

Jingyao Meng[1, 6], Yevhen Holubnyak[2], Franciszek Hasiuk[3], Jennifer Hollenbach[4], and Dana Wreath[5]
[1]*Kansas Geological Survey, University of Kansas, Lawrence, Kansas 66047, jingyao.meng@ku.edu*
[2]*Kansas Geological Survey, University of Kansas, Lawrence, Kansas 66047, eugene.h@ku.edu*
[3]*Kansas Geological Survey, University of Kansas, Lawrence, Kansas 66047, franek@ku.edu*
[4]*Kansas Geological Survey, University of Kansas, Lawrence, Kansas 66047, JHoll@ku.edu*
[5]*Berexco LLC, Wichita, Kansas 67206 dwreath@berexco.com*
[6]*Corresponding Author*

ABSTRACT

Approximately 26 square miles of new 3-D seismic data were acquired in July 2019 over the Patterson Site (Kearny County, Kansas) to assess its potential for carbon dioxide (CO_2) storage. Seismic interpretation revealed that the Patterson Site contains multiple structural closures that lie on uplifted fault blocks, bounded by two reverse faults that strike nearly perpendicular to each other. These faults offset Precambrian through Pennsylvanian sections, including several primary reservoir and seal intervals. Fault displacements are maximum at the Precambrian basement and decrease upward. Data indicated a range of structural and combination traps exists at the Patterson Site in the Cambrian-Ordovician Arbuckle through Mississippian Osagian reservoirs. The three-way closures along the NW–SE fault have structural relief of ~130 ft (40 m), and the four-way closures contain relief of ~60 ft (18 m). Erosional surfaces and multiple basement fractures also are observed on the top of the Precambrian. A Mississippian-aged incised valley system also was observed at the Patterson Site. The incised valleys formed during the Meramecian-Chesteran Stages with an incised depth up to 250 ft (76 m). The motion of the reverse faults likely captured existing meandering and linear channels, causing the current deeply incised morphology. The incised valleys observed at Patterson are similar in age, structural style, shape, incision depth, and seismic attribute properties to incised valleys observed by other workers at Pleasant Prairie South, Eubank, and Shuck oil fields (southwest Kansas). Further research should focus on estimating reactivation tendency and sealing characteristics of the reverse faults to evaluate the seal integrity of the saline reservoirs. This will reduce uncertainty concerning the risk of CO_2 migration during injection and storage. Further reservoir description, modeling, and simulation are also underway to characterize the storage potential at the Patterson Site.

INTRODUCTION

Interest is growing in carbon dioxide (CO_2) capture, utilization, and storage (CCUS) as a means to offset anthropogenic CO_2 emissions. Kansas is strategically positioned for these developments because of its central location between CO_2 producers (e.g., coal-fired power plants, ethanol distillers) and deep saline storage resources, both in the state and in nearby states (e.g., Oklahoma, Texas, and New Mexico). Numerous previous studies have evaluated technologies that could enable CCUS projects in southwestern Kansas and identified multiple geologic sites that could serve commercial-scale CO_2 storage and

Midcontinent Geoscience • Volume 1 • November 2020

Midcontinent Geoscience is an open-access, peer-reviewed journal of the Kansas Geological Survey. The journal publishes original research on a broad array of geoscience topics, with an emphasis on the midcontinent region of the United States, including the Great Plains and Central Lowland provinces.

enhanced oil recovery (EOR) (fig. 1; Dubois et al., 2015; Watney et al., 2016; Holubnyak et al., 2018, 2019, 2020). These studies included a test injection of 20,000 tonnes of CO_2 for EOR at the Wellington Oil Field, Sumner County, Kansas (Ohl and Raef, 2014; Holubnyak et al., 2017; Gupta et al., 2017); an evaluation of the regional CO_2 sequestration potential in a saline aquifer and depleted oil reservoirs, south-central Kansas (Watney et al., 2016); a test injection of CO_2 with high-resolution seismic reflection monitoring at the Hall-Gurney Oil Field, Russell County, Kansas (Miller et al., 2004; Raef, Miller, Byrnes et al., 2005; Raef, Miller, Franseen et al., 2005; Byrnes et al., 2010); and the submission of a U.S. Environmental Protection Agency (EPA) Underground Injection Control (UIC) Class VI CO_2 sequestration well permit at Wellington Oil Field, Sumner County, Kansas (Holubnyak et al., 2016).

The Carbon Storage Assurance Facility Enterprise (CarbonSAFE) program under the U.S. Department of Energy National Energy Technology Laboratory (DOE-NETL) has focused on the development of geologic sites with the capability to store at least 50 million metric tonnes (Mt) of CO_2 from industrial sources (Sullivan et al., 2019). Potential sequestration sites in the North Hugoton embayment and the Forest City basin were evaluated under a CarbonSAFE Phase I project (Holubnyak et al., 2018). The Patterson Site in Kearny County, southwestern Kansas, was identified as the most favorable site during that project. The Patterson Site is composed of three oil fields over an area of 36 mi^2 and is one of five closed geologic structures in the North Hugoton Storage Complex (NHSC). Through initial geological modeling and reservoir simulation, the Patterson Site was shown to be capable of storing at least 50 Mt of CO_2 in a set of stacked, saline, carbonate reservoirs over a 25- to 30-year injection timeframe (Holubnyak et al., 2018); recent estimates show the storage potential is more than 200 Mt. The Patterson Site, therefore, was chosen as a candidate for further reservoir characterization and modeling during a CarbonSAFE Phase II project.

A main challenge during the CarbonSAFE Phase I study was the limited availability of subsurface data (e.g., seismic data, well logs, core samples, and injectivity data) at the Patterson Site. The previous geological model was built without the advantage of having three-dimensional (3-D) seismic to delineate the overall geometry of the trap. The same lack of subsurface data left questions about the capacity of reservoir intervals and the integrity of seal intervals (Holubnyak et al., 2020). During CarbonSAFE Phase II, two new 3-D seismic surveys were acquired over the Patterson and Hartland oil fields and integrated with two legacy datasets over the Heinitz and Oslo oil fields to characterize the regional structural framework of the Patterson Site. In March–June 2020, two new deep wells were drilled to the Precambrian crystalline basement to acquire petrophysical, geomechanical, geochemical, and engineering data from core, wireline logs, and well tests. In this study, we used data from the new and legacy 3-D seismic reflection surveys to define the structural framework at the Patterson Site to reduce uncertainty regarding the potential for a CO_2 storage system at the Patterson Site. The new structural model presented herein

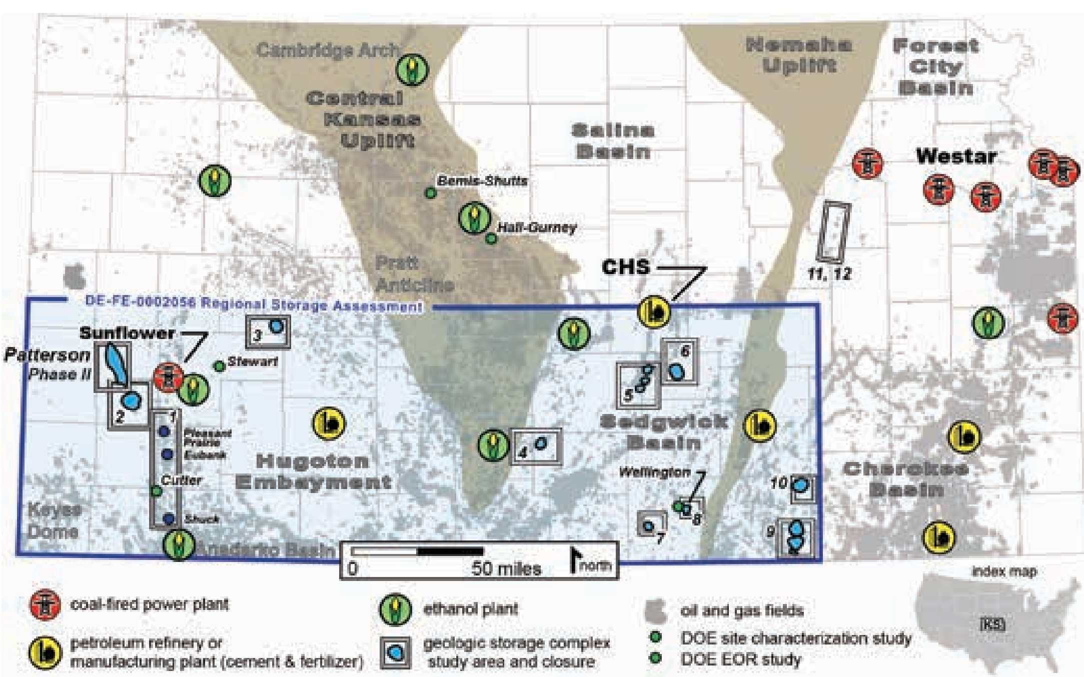

Figure 1. Kansas map showing the location and general regional structural province of the Patterson Site discussed in this study, various CO_2 sources, and other possible CO_2 injection sites in Kansas evaluated during previous CCUS projects (numbered 1–12) (modified from Holubnyak et al., 2018).

will support property modeling and reservoir simulation of CO_2 injection and storage to more accurately assess the potential of the Patterson Site for CCUS. In addition, the discovery of the Mississippian incised valley system in the new seismic data provides insight for additional sequestration and EOR potential at the Patterson Site.

GEOLOGICAL SETTINGS

Study Area

The Patterson Site lies in the Hugoton embayment of the Anadarko basin in southwest Kansas (fig. 1). The Hugoton embayment began to develop in the Cambrian-Ordovician (Rader, 1987) and became inactive by the Mesozoic (Merriam, 1963). It is bounded on the east by the Pratt anticline and the Central Kansas uplift, on the northeast by the Cambridge arch, on the west by the Apishapa-Sierra Grande uplift and the Ancestral Rockies, on the southwest by the Keyes dome, and on the south by the Anadarko basin (Youle, 1991). Strata in the Hugoton embayment include a thick succession of Paleozoic to Cenozoic siliciclastics, carbonates, and evaporites that were deposited unconformably on the Precambrian crystalline basement (figs. 2 and 3). The thickest accumulation of sediments in the Hugoton embayment occurred during the Late Mississippian through Early Permian (Youle, 1991). The Hugoton Field, which is only one of the numerous oil and gas fields in the Hugoton embayment, is the largest gas field in North America and one of the largest gas fields in the world, with original gas-in-place estimated to have been 54 trillion cubic feet (TCF; KGS, 2001, 2007). The Patterson Site is located at the northern end of the Hugoton embayment and is composed of three closely spaced oil pools (Patterson, Heinitz, and Hartland fields) aligned on a geologic structure (fig. 1). Through August 2018, a total of 7.3 million barrels of oil have been produced from Mississippian carbonates, Morrowan sandstone, and Chesteran sandstone zones of the three pools (Holubnyak et al., 2020).

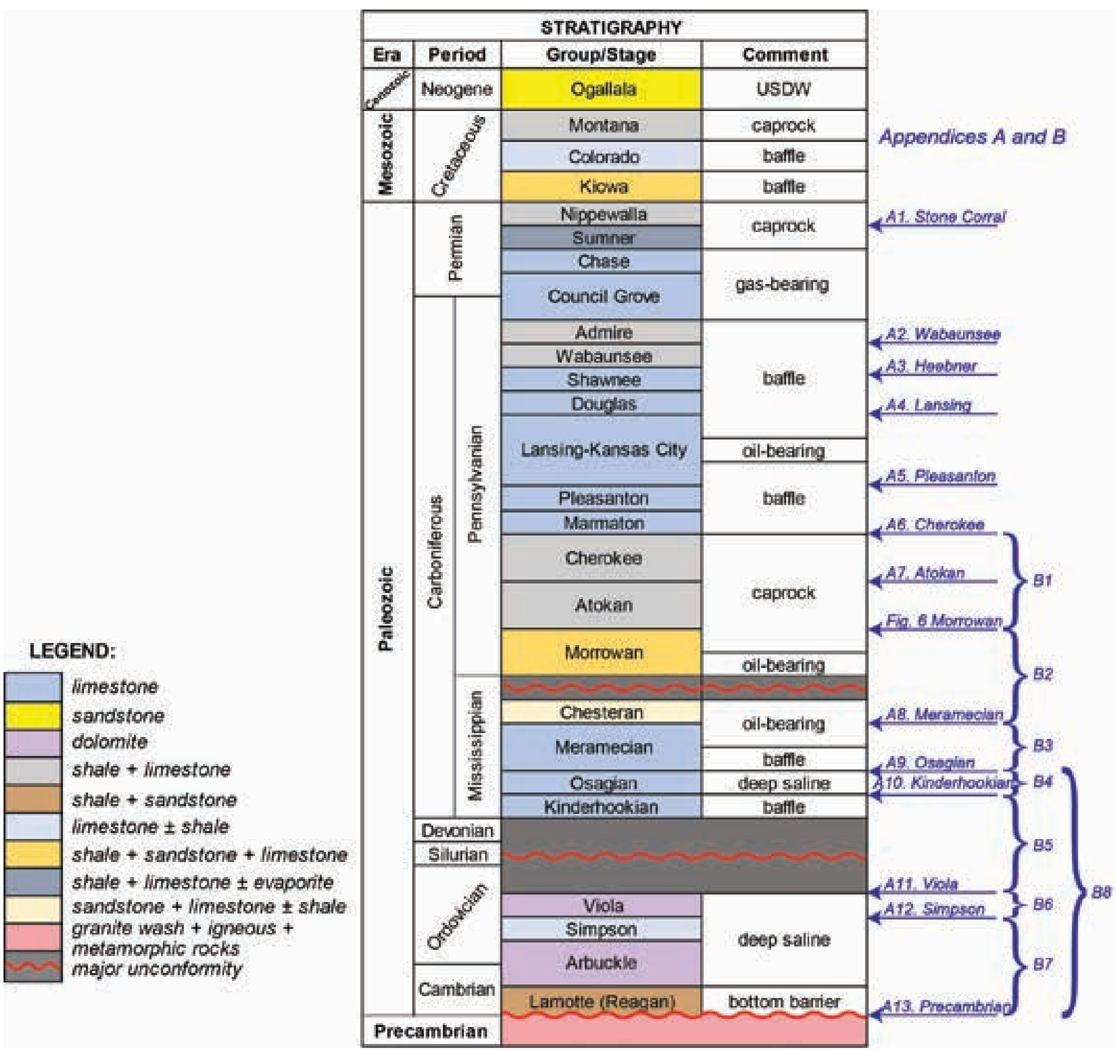

Figure 2. Generalized stratigraphic chart for the Patterson Site in southwest Kansas. The comment column shows oil and gas producing intervals in the area as well as regional barriers, caprocks, and baffles to vertical fluid flow. Structural contour and isopach map intervals in Appendices A and B are shown on the right. USDW = underground source of drinking water. (Modified from Holubnyak et al., 2018, 2020).

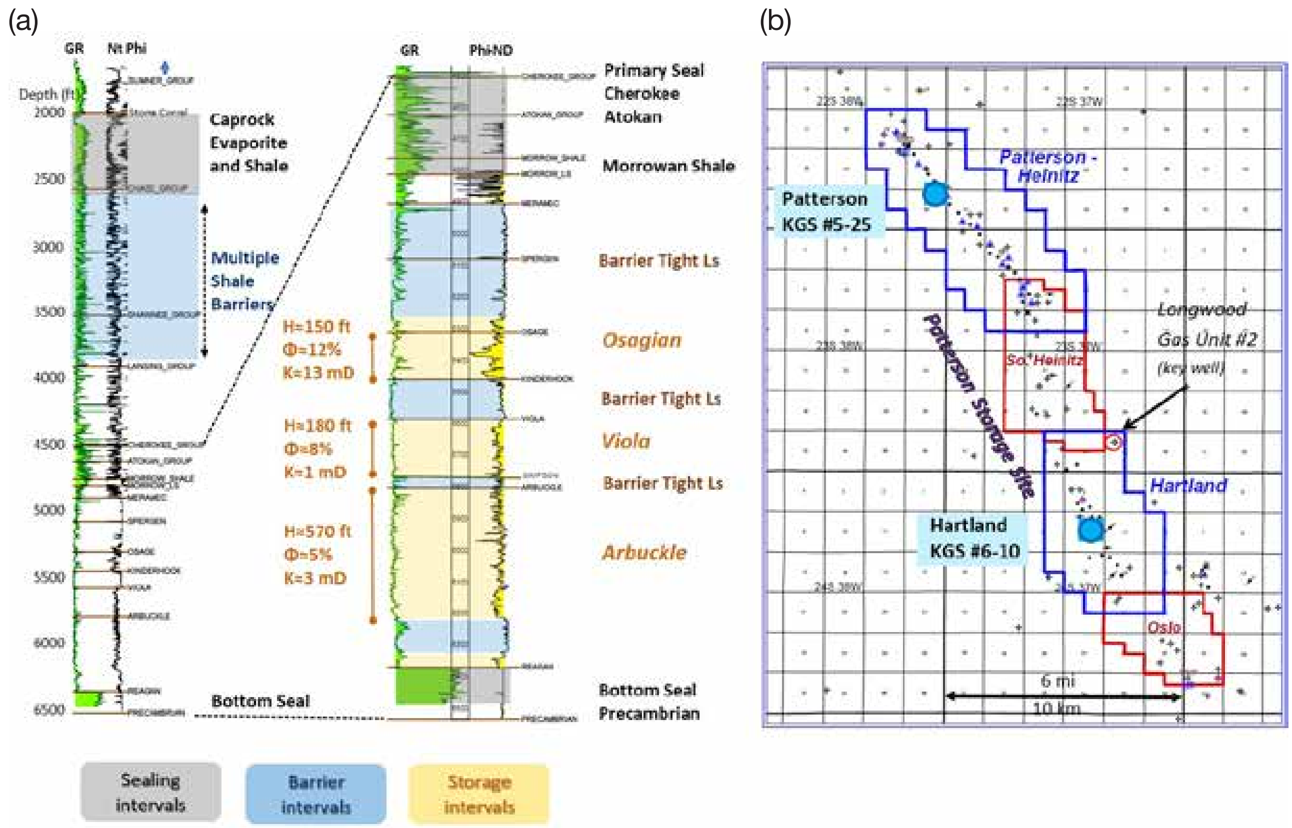

Figure 3. (a) Stratigraphy illustrated by gamma ray and neutron porosity wireline logs from a key deep well at the Patterson Site (Longwood Gas Unit #2 well, API: 15093208150000). (b) The areas for which new 3-D seismic data for Phase II were obtained are outlined in blue (Patterson-Heinitz and Hartland). Legacy 3-D shoots seismic data sites are outlined in red (South Heinitz and Oslo). Locations of two new deep wells that are also part of this study are shown as blue circles (modified from Holubnyak et al., 2018).

CO_2 Storage Reservoirs and Seals

Previous studies proposed three deep saline storage zones at the Patterson Site, including the Cambrian-Ordovician (Arbuckle), Ordovician (Viola), and Mississippian (Osagian) dolomite and cherty dolomite (fig. 3; Holubnyak et al., 2020; Watney et al., 2016). These reservoirs lie below the Hugoton Gas Field and below the oil reservoirs under current production. Potential CO_2 reservoir intervals are thick, laterally extensive, and separated by barriers to vertical fluid migration (Meramecian, Kinderhookian, and Simpson dense carbonates and shales). The shallowest reservoir is at a depth of ~4,800 ft (1,460 m). The reservoirs are under a normal hydrostatic gradient and geothermal gradient that reach the critical point of CO_2, and therefore all three reservoirs would be expected to maintain stored CO_2 in a supercritical state. Multiple regionally continuous shales in the Morrowan, Atokan, and Cherokee intervals form the primary seals for CO_2 reservoirs. Morrowan shale is also a regional top seal for oil and gas accumulations in the Mississippian, Morrowan sandstone, and Chesteran sandstone in the Hugoton Field (Newell et al., 1989). Numerous shale units are present in the Pennsylvanian-Cretaceous sections and provide secondary confining units that help ensure the containment of injected CO_2. Evaporites of the upper Permian Sumner and Nippewalla Groups form regionally extensive caprock strata that isolated the Ogallala portion of the High Plains aquifer from oil and gas development activities in the deeper subsurface for the last 90 years (fig. 2; Holubnyak et al., 2018).

Chesteran Incised Valley System

Dubois et al. (2015) performed a CO_2-EOR technical feasibility study of the Chesteran incised valley system found in three oil fields south of the Patterson Site (Pleasant Prairie South, Eubank, and Shuck oil fields; fig. 4). These three oil fields produce from Chesteran sandstone reservoirs that fill a long valley incised into the Meramecian surface. Seismic data collected over these fields showed that the deep fluvial incision formed a nearly linear, narrow, deep valley in the Meramecian surface. Based on geological modeling and simulation, these three fields were proposed as candidates for up to 100 Mt of additional CO_2 sequestration capacity concurrent with EOR potential (Watney et al., 2016; Dubois et al., 2015).

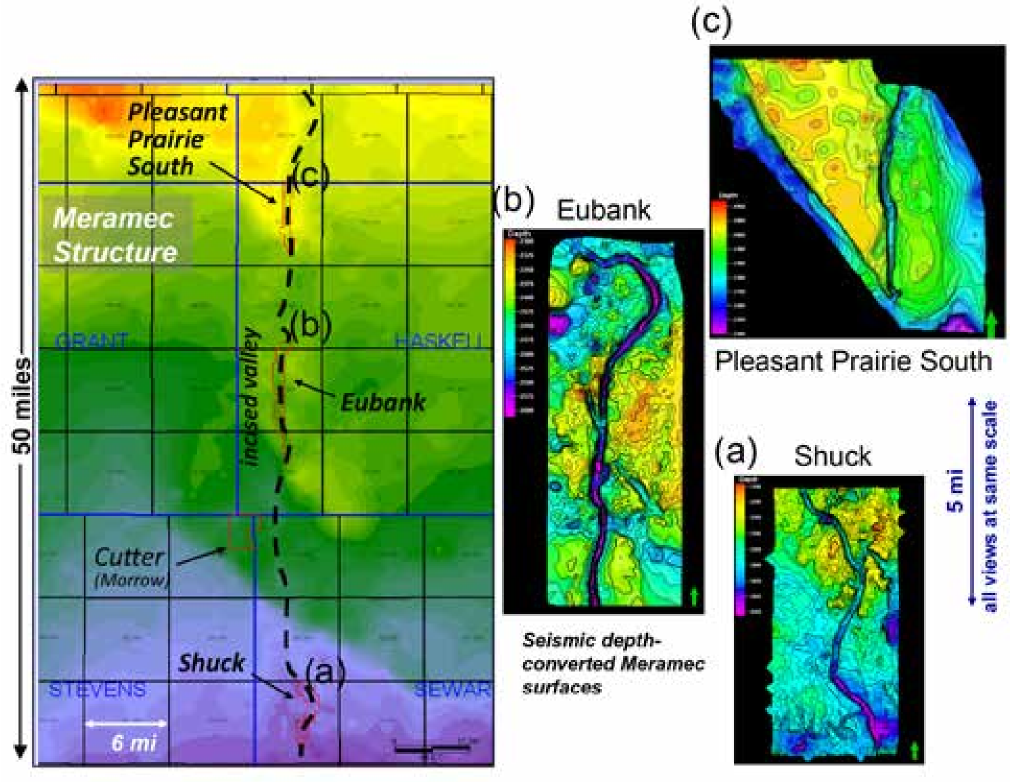

Figure 4. Location of three oil fields (Pleasant Prairie South, Eubank, and Shuck) in southwest Kansas assessed in a previous CCUS study (Dubois et al., 2015). The fields were interpreted to occupy a long valley incised into the top of the Meramecian (left). Depth structure maps (a, b, and c) for the three fields are shown on the right (modified from Dubois et al., 2015).

DATA AND METHOD

Data used for this study include P-wave 3-D seismic reflection surveys and geophysical well logs. The seismic surveys at the Patterson Site were divided into four main shoots (Patterson, Hartland, Heinitz South, and Oslo areas) and cover a total of approximately 39.6 mi^2 (fig. 3; table 1). Approximately 28.8 mi^2 of high-quality 3-D seismic data were acquired in July 2019 over the Patterson and Hartland oil fields. Another 10.8 mi^2 of legacy 3-D seismic data were acquired from operators of the Heinitz South and Oslo oil fields. In the Patterson and Hartland areas, two new deep wells — Patterson KGS #5-25 well (API: 15093219790000) and Hartland KGS #6-10 well (API: 15093219800000) — were drilled in March–June 2020 to collect wireline log data, well test data, and core material for geomechanical, reservoir, geochemical, and engineering analyses (fig. 3).

In the CarbonSAFE Phase I project (Holubnyak et al., 2018), structural and stratigraphic models were constructed from formation tops in more than 300 wells penetrating Meramecian to Precambrian strata in the vicinity of the Patterson Site. Of those wells, 108 were located within the Patterson Site and were used in this study. Formation tops from the available deep wells were used to correlate seismic amplitudes and perform a seismic-well tie using Schlumberger's Petrel software. After the seismic-well tie, 3-D seismic data were interpreted using standard sequence stratigraphic procedures. Seismic amplitude horizons from the top of the Precambrian to the Permian Stone Corral Formation evaporites were identified, correlated, and mapped throughout the study area using Petrel. Due to variation of the final seismic datum in the legacy and newly acquired poststack data volume, a time shift was applied in the legacy seismic data to best trace the seismic horizons. This also generated some artificial discontinuities in the overlapping areas of the 3-D seismic surveys. As horizons were traced, discontinuous and offset reflections were used to define bed cutoffs and major fault planes that displace the primary seal (Morrowan-Cherokee Group). Major structural features, including dipping panels, folds, and faults, were identified and characterized after depth conversion. Multiple seismic attributes were also generated to better characterize basement structures and the incised valley

Table 1. List of 3-D seismic survey sites used in this study and their areal extents.

Seismic Survey	Area (acres)	Area (mi^2)	Area (km^2)
Patterson	10,752	16.8	43.5
Heinitz South	4,720	7.4	19.2
Hartland	7,680	12.0	31.1
Oslo	3,440	3.4	8.8
Total	26,592	39.6	102.6

fill through the Petrel volume attribute function. Seismic volume attributes generated using Petrel included amplitude contrast, variance, chaos, envelope, RMS amplitude, and ant tracking (Schlumberger, 2015). Time-seismic profiles were depth-converted in Petrel using the wellbore sonic logs of the two new wells and the Longwood GU2 well at the site. Fault strike and dip data were analyzed using Stereonet software (Allmendinger et al., 2013) to generate rose diagrams and understand the mean azimuth of each fault. Depth structure maps of marker beds (Appendix A) as well as isopach maps (Appendix B) of the reservoir and primary seal intervals were constructed based on seismic horizon interpretation to characterize the regional structural framework and then modeled in 3-D using Petrel. Key parameters of the potential reservoir and seal intervals were summarized and compared with results from the CarbonSAFE Phase I stratigraphic model (tables 2–4). The updated static geological model will be used for distributing rock properties (e.g., porosity, permeability) within the reservoir and seal intervals away from well control after adding the lithological and petrophysical information from the two new deep wells.

RESULTS

Seismic Interpretation

Figure 5 shows an example interpreted seismic line at the Patterson Site, fig. 6 shows the location for the seismic line, and Appendix C shows the seismic-well tie detail. The Patterson and Hartland 3-D seismic data are of good quality with little evidence of noise contamination and broad frequency content (~15 Hz – 60 Hz). Synthetic seismic tie to wells indicates nearly reverse polarity data. The Precambrian crystalline basement generally contained chaotic and nonparallel reflections; weakly divergent reflections are shown below the Precambrian surface lumped with Lamotte (Reagan) Sandstone, which itself was marked by a distinct, continuous, high-amplitude reflection (~-1,120 ms two-way time [TWT]). The top of the Cambrian-Ordovician Arbuckle Group dolomite was characterized by a discontinuous, moderate- to low-amplitude reflection (~-1,045 ms

Table 2. Summary of depth and elevation of the top of each reservoir interval. TVD: total vertical depth.

Reservoir depth (ft)	Arbuckle		Viola		Osage	
	Elevation	TVD	Elevation	TVD	Elevation	TVD
Max.	-3,482	6,732	-3,023	6,273	-2,692	5,942
Min.	-2,179	5,429	-2,042	5,292	-1,867	5,117
Mean	-2,628	5,878	-2,402	5,652	-2,134	5,384
Std. Dev.	182		169		170	

Table 3. Summary of the thickness of reservoirs and primary seals at the Patterson Site.

Reservoir/seal Thickness (ft)	Arbuckle	Viola	Osage	Meramecian	Morrowan	Atokan-Cherokee
Max.	1,023	444	481	855	402	298
Min.	446	84	0	209	51	109
Mean	671	225	144	462	134	223
Std. Dev.	113	43	82	94	54	15

Table 4. Comparison of three reservoir intervals with the previous stratigraphic model (Holubnyak et al., 2018).

	Phase I		Phase II	
	Depth (ft)	Thickness (ft)	Depth (ft)	Thickness (ft)
Osage	5,260–5,400	150	5,114–5,942	144
Viola	5,500–5,700	180	5,292–6,273	225
Arbuckle	5,740–6,340	570	5,429–6,732	671

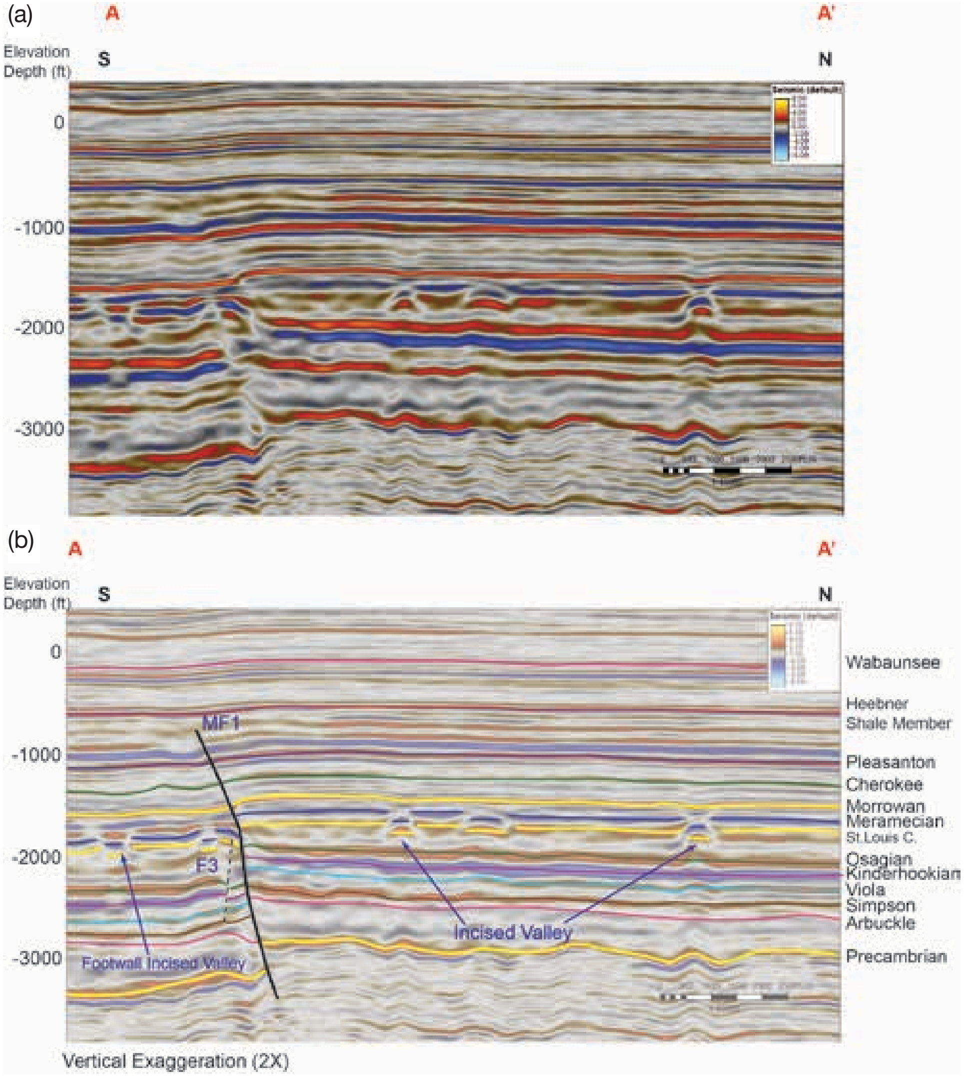

Figure 5. Uninterpreted (a) and interpreted (b) seismic line (A–A'; Patterson IL120); see fig. 6 for location.

TWT). This discontinuous reflection was overlain by a continuous, high-amplitude reflection marking the top of the Simpson Group, which could be traced through much of the study area. Therefore, in this study, we used the top of the Simpson Group (~-1,035 ms TWT) to compute the thickness of the Arbuckle Group potential reservoir. Results from coring, otherwise beyond the scope of this study, support this assumption, showing no typical Simpson lithology (i.e., shale) at the top of the Arbuckle. A continuous, moderate- to high-amplitude reflection corresponded to the top of the Viola Limestone (~-1,025 ms TWT). The top of the Kinderhookian was identifiable as a regional, continuous, low-amplitude reflection (~-1,005 ms TWT). The top of the Osagian limestone formed a continuous, high-amplitude reflection (~-995 ms TWT). The principal intervals evaluated for CO_2 storage potential were within the Arbuckle, Viola, and Osagian sections. A continuous, high-amplitude reflection corresponding to the top of the St. Louis Limestone defined the base of the incised valleys that underlie the Mississippian-Pennsylvanian unconformity (top Meramecian Group low-amplitude reflection; ~-950 ms TWT). Chesteran-age rocks fill the incised valley. The Morrowan shale is a regional marker bed and formed a continuous, high-amplitude reflection (~-920 ms). Above the Atokan Stage continuous, low-amplitude horizon (~-900 ms TWT), the top of Cherokee sediments formed a continuous, moderate- to high-amplitude reflection (~-885 ms TWT). In the upper Pennsylvanian section, the Pleasanton Group contained a continuous, high-amplitude reflection (~-865 ms TWT). The top of the Lansing Group formed a continuous, high-amplitude reflection (~-805 ms TWT). The Heebner Shale Member (Shawnee Group) formed a continuous, low-amplitude reflection (~-795 ms TWT), and a continuous high-amplitude reflection corresponded to the top of the Wabaunsee Group (~-705 ms TWT). The evaporites of the Stone Corral Formation constitute a regional marker bed and formed a robust, continuous, high-amplitude reflection in seismic (~-505 ms TWT). The Stone Corral Formation marks the top of the Permian Sumner Group and is the final top mapped as part of this study.

Structural Framework

Based on the seismic interpretation, two major reverse faults were identified at the Patterson Site, termed Main Faults 1 and 2 (MF1 and MF2, respectively). Fault propagation folding on the hanging wall formed three-way structural closures aligned along MF1, which strikes N 33° W and dips at 60°–65° to the northeast (fig. 7). The depth relief from the crest of the closure is approximately 130 ft (40 m) at the Morrowan top. Multiple, small four-way closures with a relief of approximately 60 ft (18 m) were also observed in the Hartland area. The NW–SE striking fault (MF1) was present throughout the Patterson Site and therefore is the most significant fault affecting the storage site. The length of MF1 extends from the Patterson to Oslo area (~15 mi [24 km]), and depths range from 1,900 to 3,010 ft (579 to 917 m). Overall, displacement of MF1 is greatest in the Hartland area and smallest in the Oslo area (fig. 6).

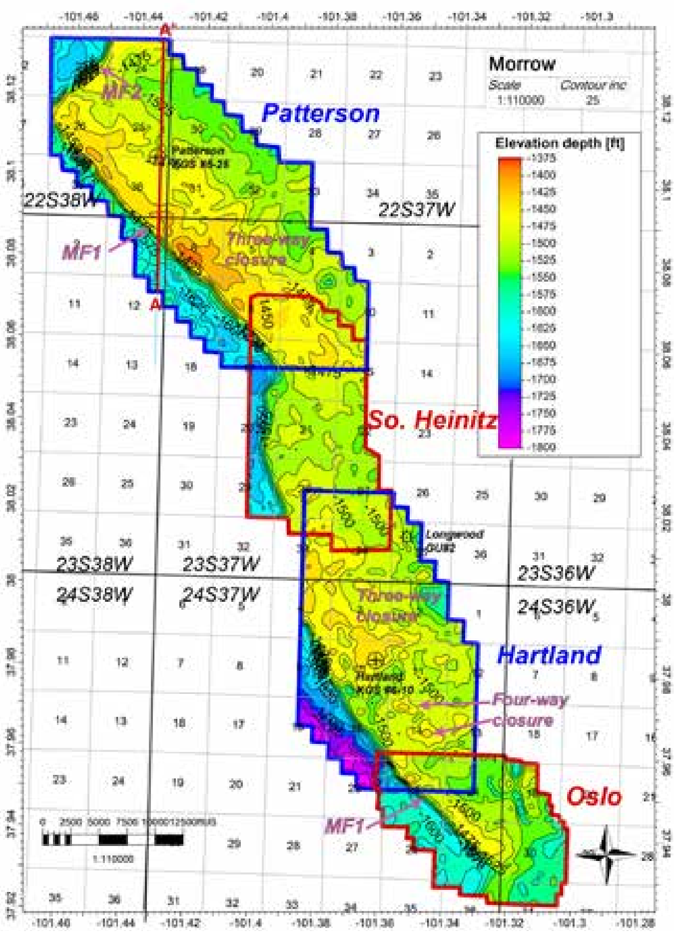

Figure 6. Depth structural contour map of the top of the Morrowan shale, showing the configuration of the primary seal in the Patterson–Oslo area (contour interval is 25 ft) and location of seismic line (A-A'; Patterson IL120).

Fault displacement decreases upward. For example, in the Patterson area, throw is 390 ft (119 m) at the top of the Lamotte (Reagan) Sandstone, ~330 ft (101 m) at the top of the upper Arbuckle Group, ~300 ft (91 m) at the top of the Viola Limestone, and ~250 ft (76 m) at the top of the Osagian, which are the target reservoir intervals. Most faults terminate near the top of the Pleasanton Group, above the primary and secondary seal intervals (fig. 5). Another major fault (MF2) strikes N 40° E and dips at 55°–65° to the southeast (fig. 7). Similar to MF1, the fault throw of MF2 decreases upward until the Pleasanton Group. The fault throw is 320 ft (98 m) at the top of the Lamotte (Reagan) Sandstone, ~230 ft (70 m) at the top of the upper Arbuckle Group, ~200 ft (61 m) at the top of the Viola Limestone, and ~150 ft (46 m) at the top of the Osagian in the Patterson area.

The major faults penetrate the strata from the Precambrian basement to nearly the mid-Pennsylvanian and offset the potential reservoir and seal intervals. The two major faults are nearly perpendicular to each other at the northwest edge of the Patterson area and form an overall uplifted block, which represented the dominant structure style of the Precambrian basement. The uplifted block maintained this configuration until the Stone Corral Formation of the Sumner Group (Appendix A). Two fault growth events are observed in the footwall strata, according to the computed isopach maps (Appendix B), including Precambrian-Simpson and Meramecian-Morrowan age. The Precambrian basement underlying the Patterson Site has a regional dip of 1.5° toward the northeast and an average structural relief of ~320 ft (98 m). The basement surface is erosional (fig. A13 in Appendix A). In addition to the major faults described above, multiple smaller faults and fracture swarms were observed in 3-D seismic volume attribute time slices close to the top of the basement. Basement faults and fracture swarms are delineated in the high variance zone (fig. 8b, e) and highlighted in ant tracking discontinuities (fig. 8c, f). Most

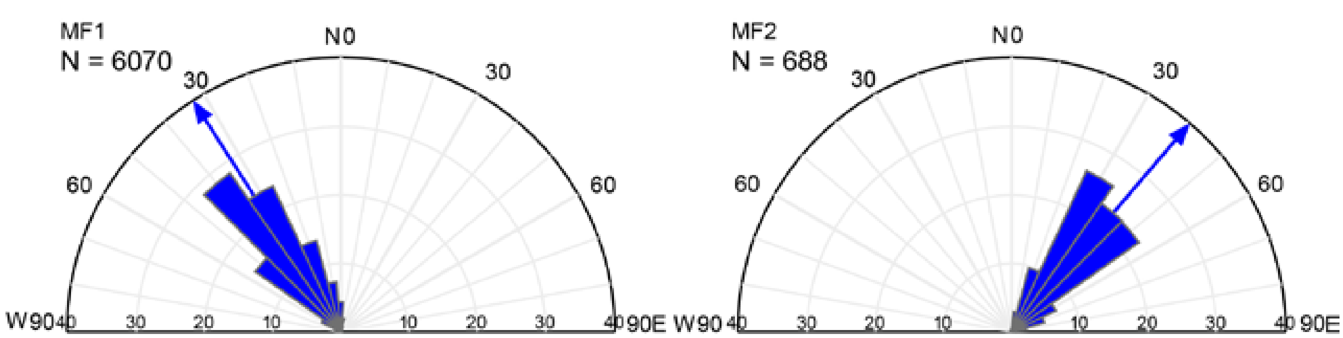

Figure 7. Rose diagrams of the fault strikes of MF1 and MF2.

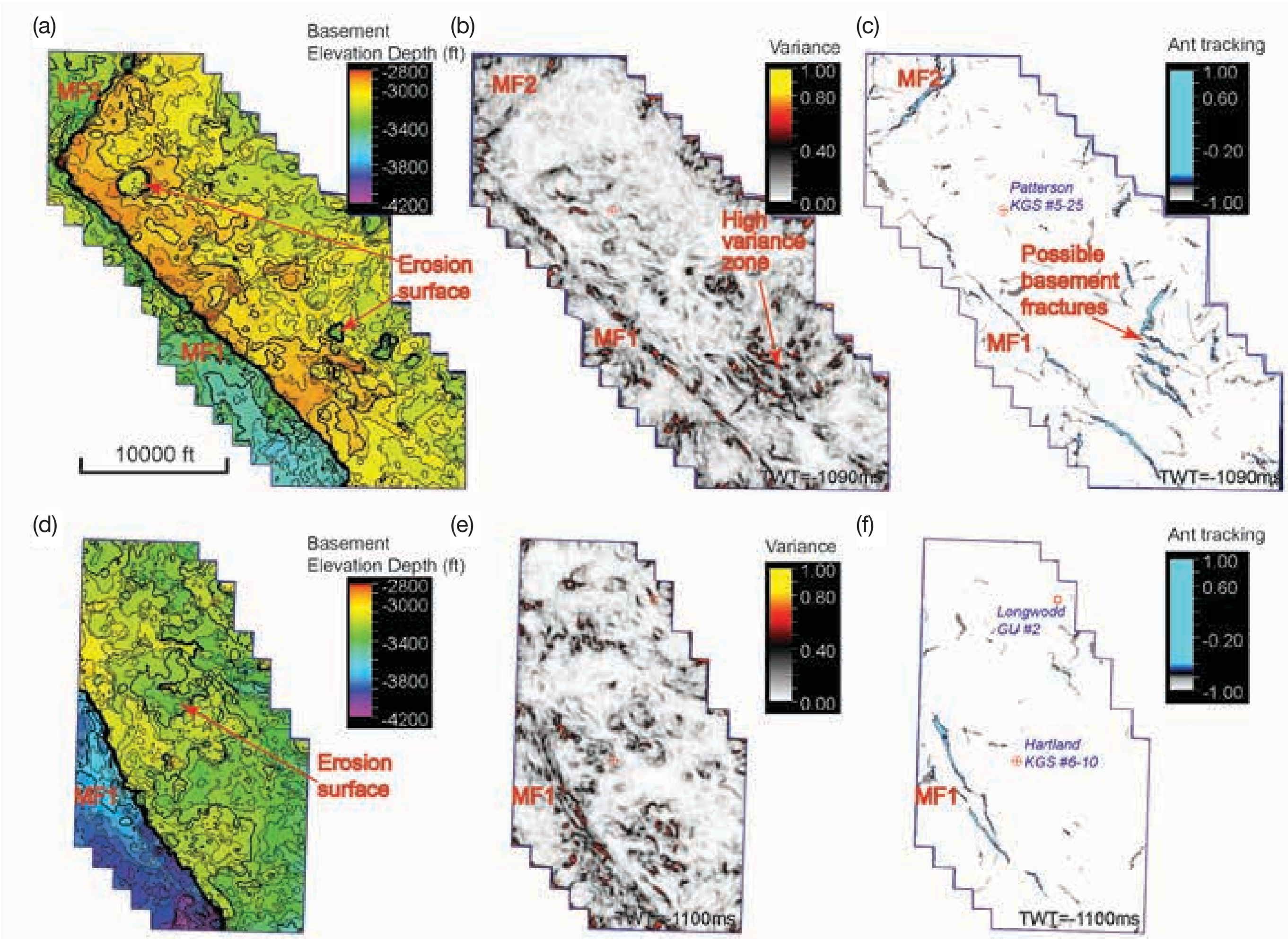

Figure 8. Seismic attribute maps of the Precambrian basement: (a) depth structure contour map of the top of the Precambrian basement (Patterson area) showing the structural framework and erosional features; contour interval is 50 ft (15 m); (b) time slice of the variance volume attribute showing a high variance cluster indicating a highly fractured surface; (c) time slice of ant-tracking volume attribute showing possible basement fractures; (d) depth structure contour map of the top of the Precambrian basement (Hartland area); contour interval is 50 ft (15 m); (e) time slice of variance volume attribute of the basement in the Hartland area; (f) time slice of ant-tracking volume attribute of the basement in the Hartland area.

of the basement fractures terminate near the top of the Precambrian and trend NW–SE, although some NE–SW oriented fractures also are present.

Maps and model

Based on the newly acquired seismic data, depth structural maps were contoured from the basement to the top of the Stone Corral Formation seismic horizons (table 2; Appendix A). Isopach maps of the three reservoirs and primary seals were computed based on the depth structural maps, including the Arbuckle, Viola, and Osagian reservoir intervals and the Meramecian, Morrowan, and Atokan-Cherokee seal intervals (table 3; Appendix B). Table 3 summarizes the thickness of each reservoir and primary seal interval. A new structural model was constructed using the depth structural maps (fig. 9). This updated structural model will be used for property modeling (e.g., porosity and permeability) of the reservoir and seal intervals in the Patterson Site after adding the lithological and petrophysical information from the two new deep wells.

Incised Valley System

An incised valley system was identified in the seismic data across the Patterson Site (fig. 1). Seismic data are of high quality in the time range (944–980 ms) of the feature. Seismic profiles defined the bottom of the incised valley as occurring at the Mississippian St. Louis Limestone and the top at the Morrowan-Chesteran unconformity (fig. 5). Seismic attribute analysis was used to explore the nature of the incised valley features in the 3-D seismic time slice at the Patterson and Hartland areas (figs. 10 and 11). The valley showed deeper incision near MF1 and exhibited a

"V" shape, including a NE–SW oriented linear valley and a NW–SE oriented meandering valley (fig. 10a). Multiple closed depressions in the regions outside the valleys are likely caused by karst dissolution (fig. 10a–b). The straight valley likely represented a fluvial channel taking advantage of a pre-existing fault (F3) that was striking NE–SW, parallel to MF2 (figs. 5 and 10). The incised valley system exists on both the hanging wall and footwall of MF1 with a thickening on the footwall strata (fig. 10b; figs. B2 and B3 in Appendix B), which confirms that the incised valleys coincide with fault movement. Depth structure mapping at the top of the Meramecian (fig. 10e) showed the depth of the valleys is up to ~250 ft (76 m).

The Hartland seismic survey also showed multiple incised valley features, including a linear valley and a partial meandering valley (fig. 11). The incised valley system is not as well expressed as it is at Patterson because most of the Hartland valleys are not as deeply incised, averaging only ~110 ft (34 m). Multiple attributes —

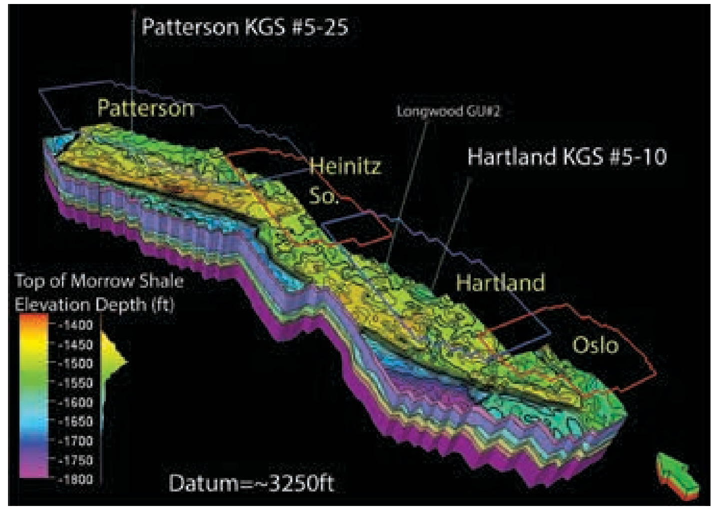

Figure 9. Structural model in the Patterson–Oslo area, showing the elevation of the top of the Morrowan shale as well as a legacy deep well (Longwood Gas Unit #2) and two new deep wells (Patterson KGS #5-25 and Hartland KGS #6-10). On the right side of the legend is a histogram of elevation depths for the Morrowan shale top.

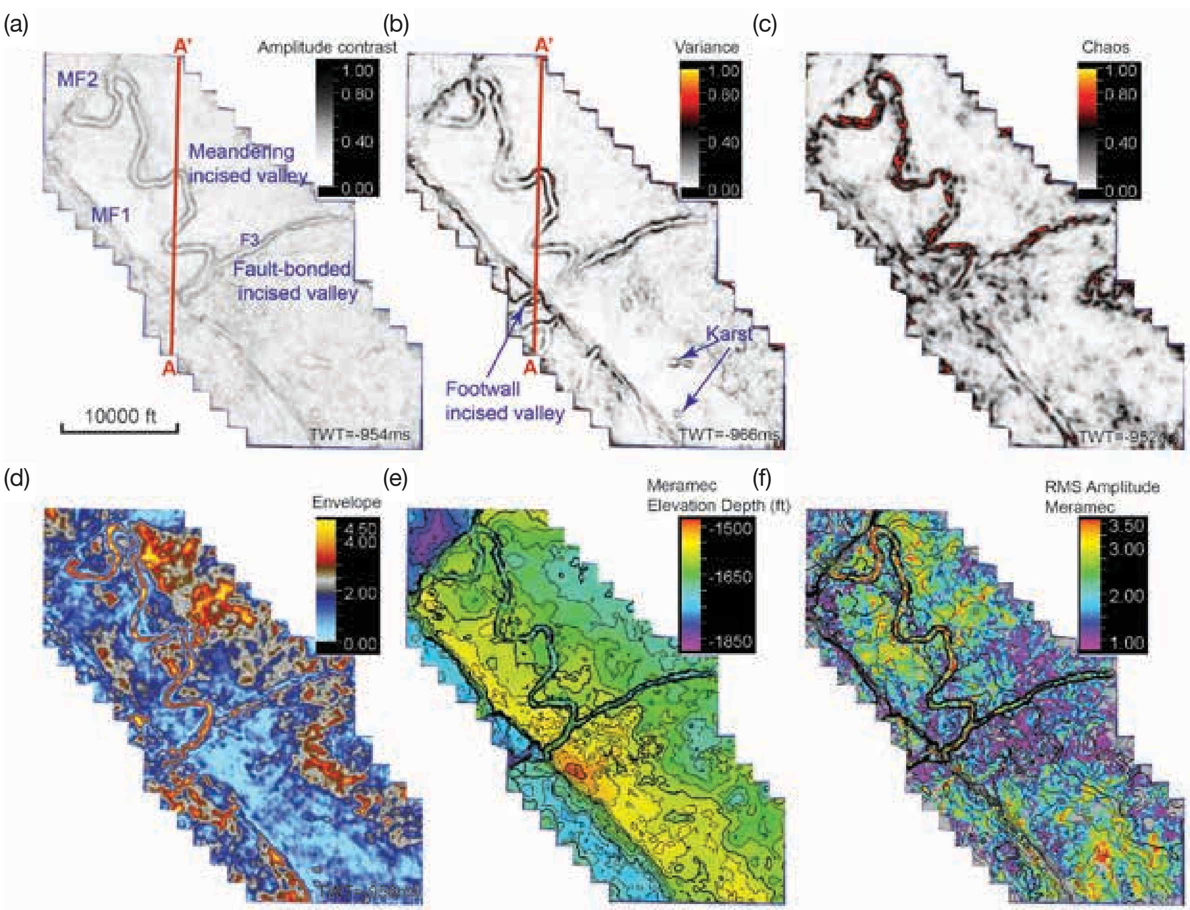

Figure 10. Seismic attribute maps of the incised valley fill in the Patterson area: (a) time slice of amplitude contrast volume attribute showing the two branches of an incised valley; (b) time slice of variance volume attribute showing the footwall of the incised valley and karst features in the Meramecian carbonate; (c) time slice of chaos volume attribute showing the amplitude contrast within the incised valley; (d) time slice of envelope volume attribute showing the amplitude contrast within the incised valley; (e) depth structure map of the top of the Meramecian; (f) RMS amplitude surface attribute map of the top of the Meramecian showing the amplitude contrast within the incised valley.

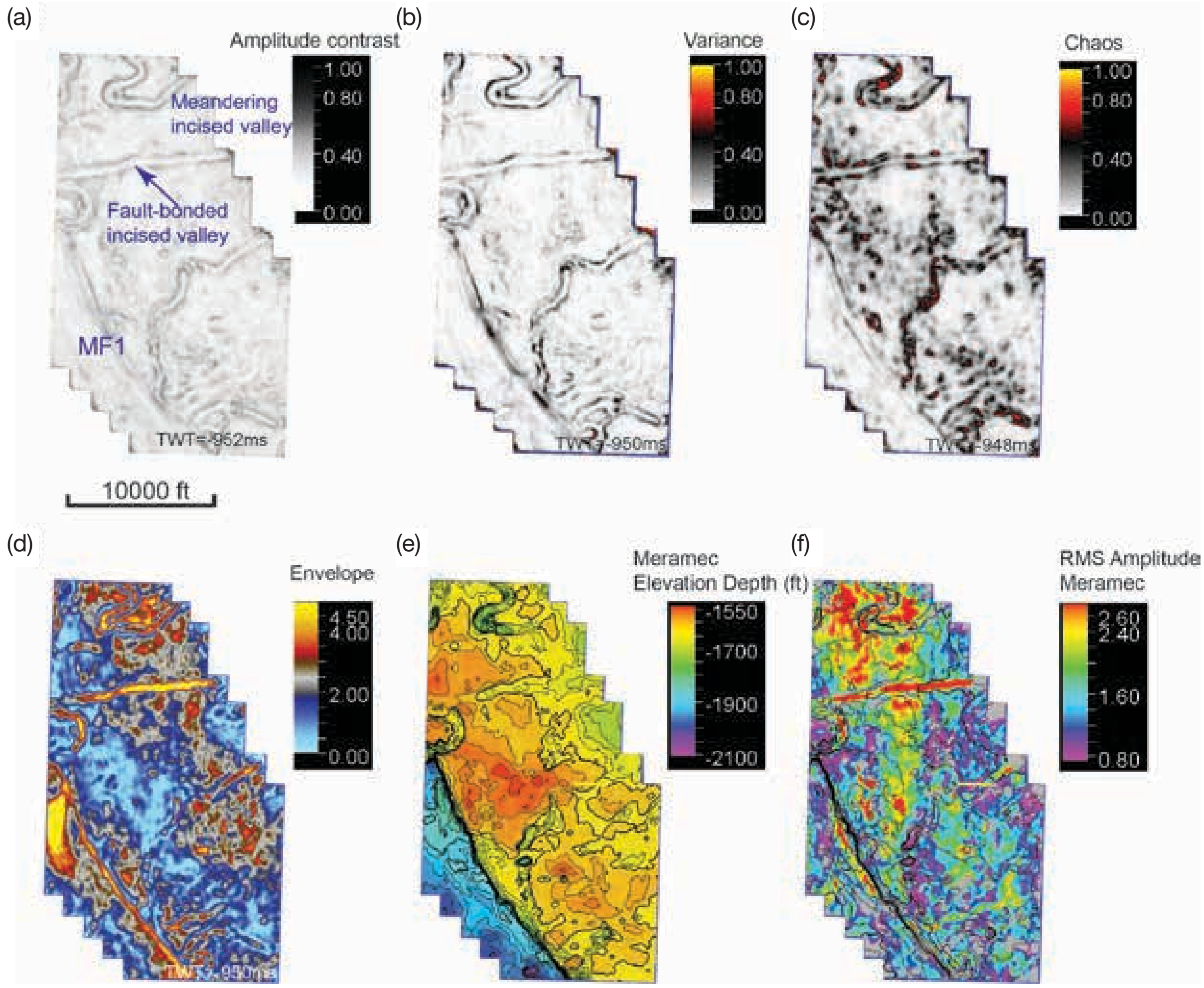

Figure 11. Seismic attribute maps of the incised valley fill in the Hartland area: (a) time slice of amplitude contrast volume attribute showing the two branches of an incised valley; (b) time slice of variance volume attribute; (c) time slice of chaos volume attribute showing the amplitude contrast within the valley; (d) time slice of envelope volume attribute showing the amplitude contrast within the incised valley; (e) depth structure map of the top Meramecian; (f) RMS amplitude surface attribute map of the top Meramecian showing the amplitude contrast within the incised valley.

including amplitude contrast, variance, chaos, envelope, and RMS amplitude — provide details that can be useful in better characterizing compartmentalization (figs. 10 and 11). Due to the variability in rock properties that likely exists between the incised bedrock (carbonate) and channel fill (siliciclastic), a significant amplitude contrast was observed between four of the time seismic horizons of volume attribute within the valley fill (figs. 10a–d and 11a–d). This contrast also can be observed in the RMS amplitude map of the top Meramecian surface (figs. 10f and 11f).

DISCUSSION

Storage System Elements

Hydrocarbon systems are often characterized based on "play system elements": source, migration, trap, seal, reservoir, and timing. In the context of subsurface CO_2 storage, source, migration, and timing have no geological meaning because the CO_2 is generated and enters the system externally from human activity. Trap, seal, and reservoir can be characterized identically, and of these, seismic data speak most directly to trap and seal.

Trap. Structural style is an essential consideration for selecting sites for CO_2 storage because style affects the size and shape of subsurface traps and the configuration of their compartments. Data indicate a range of structural and combination traps exists in the Patterson Site. Three- and four-way structural closures (fig. 6) are the dominant trap types in the area and generally are considered to be the most favorable structural trap configurations for CO_2 storage (Metz et al., 2005). The hydrocarbons in the Morrowan sandstone reservoir are able to be trapped by structural relief and the top seal on three sides of the trap and by a sealing fault on the fourth side, thus indicating the prospective trap capacity for the injected CO_2 in the deeper Arbuckle-Osagian reservoirs. Additional potential combination traps may be associated with updip pinch-out of the three reservoirs on the flanking beds of the reverse fault. Three reservoir intervals are separated by dense carbonate and thin shales from the Meramecian, Kinderhookian, and Simpson, which can form vertical barriers to trap the injected CO_2.

Seal. The potential storage reservoirs are intercalated with and overlain by thick successions of shale and nonporous carbonate, which form baffles, barriers, and seals to lateral and vertical fluid flow. Previous stratigraphic analysis (Holubnyak et al., 2018) showed that Morrowan shale formed the top seal as the principal confining unit for CO_2 storage. Numerous shale units in the Atokan Stage and Cherokee Group provide secondary confining units to ensure the containment of injected CO_2. The seismic interpretation presented here confirmed that all proposed reservoirs are below several laterally continuous sealing stratigraphic units. The nonporous carbonate of the Meramecian is thick (~462 ft [141 m]), is regionally extensive, and immediately overlies the Osagian, which is the uppermost of the three reservoirs. Morrowan shale and nonporous carbonate are also regionally extensive (as evidenced by a strong reflection throughout the combined seismic data sets) and have an average thickness of 134 ft (41 m). The superjacent Atokan-Cherokee Group, a shale-nonporous carbonate section, has been interpreted as uniformly thick (~223 ft [68 m]) throughout the study area and potentially further reduces the risk of leakage. Also, oil and gas production from Morrowan sandstone across the Patterson, Hartland, Heinitz, and Oslo fields suggests that the Patterson Site is effectively sealed against at least the upward flow of oil. In addition, the presence of the largest gas field in North America above the oil-producing Morrowan intervals is testament to the sealing quality of the upper Permian units at the Patterson Site to the upward flow of gaseous hydrocarbons. Although the properties of supercritical CO_2 are different from either oil or gas, supercritical CO_2 is likely to be sealed by the same intervals that seal these economic deposits of oil and gas.

Nevertheless, the faults at the Patterson Site still pose a risk for cross-formational migration of CO_2. Two major faults intersect the strata from the basement to the Pennsylvanian Pleasanton Group and offset the Mississippian saline reservoirs and their primary seal. The NE–SW trending incised valley system crosses an existing fault. Multiple fractures are observed in the basement surface, which may affect the integrity of the bottom seal. During injection, increasing pore pressure will increase the tendency of an existing fault and associated fractures in the caprock to slip or dilate, thereby forming a potential fluid migration pathway (Hawkes et al., 2005). Therefore, future studies should perform fault reactivation tendency analysis to understand the likelihood of dilation or slip along existing fractures. A fault is potentially sealed when a reservoir unit is juxtaposed with shale, tight limestone, evaporite, or clay gouge (Yielding et al., 1997). Although the Morrowan sandstone oil and gas reservoir is trapped by the fault, it is unknown whether the fault is acting as a migration pathway or a fault seal for trapping the CO_2 for the Arbuckle, Viola, and Osagian reservoirs. Detailed analyses of the basement fracture network, fault reactivation tendency, and fault seal are recommended in future research to provide an integrated seal evaluation to understand the fault sealing characteristics of those saline reservoirs.

Reservoir. Isopach maps further refine the CarbonSAFE Phase I estimates (Holubnyak et al., 2018) of reservoir distribution and quality of the three storage targets (table 4). The Phase I study estimated that the Arbuckle reservoir was 570 ft (174 m) thick. Based on our study, the Arbuckle is 600–800 ft (183–244 m) thick in the Hartland-Oslo area and thins toward the Patterson area to ~500 ft (152 m). The average vertical thickness of the Arbuckle reservoir is approximately 670 ft (204 m) (fig. B7 in Appendix B). Due to the difficulty in identifying the top of the Arbuckle mentioned above, the computation of the Arbuckle Group included the overlying Simpson Group and the underlying Lamotte (Reagan) Sandstone. Therefore, it is expected that the Arbuckle reservoir interval in the structural model is thicker than the previous stratigraphic model. The Viola Limestone contains an average vertical thickness of 225 ft (69 m) of dolostone at the Patterson Site. The isopach map of the Viola Limestone indicated a relatively uniform reservoir rock with some thickening to the north (fig. B6 in Appendix B). The Osagian Stage is the shallowest and thinnest of all the three potential CO_2 storage targets. Similar to the Arbuckle Group, the Osagian isopach map (fig. B4 in Appendix B) shows the vertical reservoir thickness thinning at the northwest edge of the Patterson area, in this case down to 30–60 ft (9–18 m).

The estimated average thickness of the three reservoir intervals agrees with the stratigraphic model produced from the previous study (Holubnyak et al., 2018). Overall, the south of the Patterson Site provides more net reservoir thickness than the north (fig. B8 in Appendix B). Future work will incorporate the reservoir data from the two new wells to more accurately assess the potential of the Patterson Site for CCUS.

Structural Styles and Incised Valley System Comparison in Adjacent Areas

3-D seismic interpretation corresponds with the observations from seismic datasets in adjacent areas in southwest Kansas (Dubois et al., 2015; Holubnyak et al., 2018). Previous studies indicated that most faults and fault blocks in southwest Kansas oil fields are oriented NW–SE; however, N–S to NE–SW oriented structures also are present (Dubois et al., 2015). Similarly, a NW–SE oriented major fault (MF1) and basement fracture swarms were recognized and dominate the structural style in our study area. We also observed two NE–SW oriented faults (MF2 and F3) and other basement fracture swarms. The two major faults offset the strata from the Precambrian basement into the Pennsylvanian but are overlapped by a mid-Pennsylvanian horizon, suggesting fault motion predates that surface. We observed footwall growth strata in both the Precambrian-Simpson isopach map and Meramecian-Morrowan isopach map (figs. B2, B3, and B7 in Appendix B), suggesting two phases during which the sedimentary section responded to reactivation of existing Precambrian basement faults. Similar agreement was recognized for the Shuck, Cutter, Eubank, and Pleasant Prairie South fields of southwest Kansas (Dubois et al., 2015). In contrast with our study area, most of the near-vertical faults in the Wellington Oil Field of south-central Kansas are oriented NNE (Schwab et al., 2017). Unlike at the Patterson Site, where faults offset the basement to Pennsylvanian sections, the Wellington Field faults offset the basement but terminate before the top Mississippian. Considering the dissimilarity of the fracture orientation and offsetting stratigraphic intervals between the Patterson and Wellington areas, the structural styles at these two sites appear to have different tectonic origins.

The incised valley system in the Patterson Site is a new interpretation. The existence of a Mississippian incised valley system at the Patterson Site was not identified previously because there was no seismic coverage of the area. Seismic interpretation of the incised valley system is similar to that of a previous study in the Shuck, Eubank, and Pleasant Prairie South oil fields that the deep incision formed on the Meramecian surface (Dubois et al., 2015). The NW–SE trending incised valley observed at the Patterson Site was more sinuous than the valleys in the Shuck, Eubank, and Pleasant Prairie South fields (fig. 10). The linear incised valley observed in the Patterson area is more consistent with the valley at Pleasant Prairie South (figs. 4 and 9). Without wells that directly penetrate the incised valley, we only have the opportunity to observe a significant impedance contrast to estimate rock properties. Meramecian rocks are higher density carbonates, while the overlying Chesteran series are lower density shales and sandstones with highly variable velocity compared to the more regular velocities within the Meramecian (Dubois et al., 2015). The incised valley system in the Patterson Site and the four other fields is likely part of a regional fluvial system. In the Shuck, Eubank, and Pleasant Prairie South oil fields, oil is produced from the Chesteran sands, suggesting that in the Patterson Site the incised valleys might be prospective intervals for hydrocarbon production as well as CO_2 storage and EOR. Neither of the two deep wells drilled for this project targeted these incised valley fills. However, several wells have been drilled previously as part of the development of hydrocarbon resources at the Patterson, Hartland, and Heinitz fields. The examination of cuttings from these wells may provide sufficient information for reservoir characterization, modeling, and simulation of the Chesteran incised valley fill reservoirs in the Patterson Site to understand the deposition history of this fluvial system and quantify the potential for gas storage and EOR.

CONCLUSIONS

Newly acquired 3-D seismic reflection surveys allowed more accurate definition of the structural model (i.e., traps and seals) at the Patterson Site. In addition, a new element of the stratigraphic model—namely a meandering valley system incised into the Meramecian surface—was discovered.

Two major reverse faults at the Patterson Site offset the reservoir and seal intervals and constitute an uplifted block in the Patterson area. Fault displacements are maximum at the Precambrian basement and decrease upward. Fault propagation folding on the hanging wall forms structural closures striking parallel to the NW–SE trending fault. Identified three- and four-way structural closures at the Patterson Site can assist in trapping CO_2 in the Arbuckle-Osagian reservoirs. Additional potential combination traps may exist at the updip pinch-out of the three reservoirs on the flanking beds of the reverse faults. Erosional surfaces and multiple basement fractures are observed in the 3-D seismic maps at the Precambrian top. Most of the basement fractures are trending NW–SE and terminate near the top of the basement.

We identified an incised valley system for the first time in the Patterson area. Those incised valleys form from the Mississippian St. Louis Limestone (Meramecian Stage) to the Chesteran Stage. The incised valleys show two morphologies, meandering and linear, and are incised into the Meramecian surface up to 250 ft (75 m). The incised valleys appear to cross the major fault in the area, suggesting that they coincide with the fault motion. The linear incised valley also appears to be influenced by the NE–SW trending reverse faults.

The Patterson incised valleys are similar in morphological properties to incised valleys observed in 3-D seismic in the Pleasant Prairie South, Eubank, and Shuck fields at the same stratigraphic position, suggesting they formed by the same fluvial system of Meramecian-Chesteran age. Structural styles correspond with observation from the seismic datasets in adjacent areas. A comparison of reservoir depth and thickness from our seismic interpretation shows the estimated average thickness of the three reservoir intervals agrees with the stratigraphic model from the CarbonSAFE Phase I study (Holubnyak et al., 2018).

Further research should focus on fault reactivation tendency and fault sealing characteristics of existing faults to evaluate the reservoir seal integrity of the saline reservoirs, thus reducing the risk of gas migration from the CO_2 storage complex. Reservoir characterization, modeling, and simulation for the incised valley system are also required in a future study to accurately assess the storage potential the incised valleys may provide at the Patterson Site.

ACKNOWLEDGMENTS

This work is supported by the Integrated Midcontinent Stacked Carbon Storage Hub Phase II, which is funded by the U.S. Department of Energy National Energy Technology Laboratory under cooperative agreement DE-FOA-0001450. The authors thank Merit Energy Company for providing the legacy 3-D seismic data in the study area. We thank Dr. George Tsoflias and Mr. Luke Kingsley of the Department of Geology at the University of Kansas for the advice on the seismic data description and synthetic. The authors also thank collaborators at the Kansas Geological Survey, Improved Hydrocarbon Recovery LLC, Battelle Memorial Institute, and Berexco LLC for their support on various technical issues in this paper. The authors also thank the reviewers, whose comments substantially improved the quality of this contribution.

REFERENCES

Allmendinger, R. W., Cardozo, N. C., and Fisher, D., 2013, Structural Geology Algorithms: Vectors & Tensors: Cambridge, England, Cambridge University Press, 289 p.

Byrnes, A., Willhite, G. P., Green, D., Pancake, R., Tsau, J. S., Watney, W. L., Doveton, J., Guy, W., Reynolds, R., Murfin, D., Daniels, J., Martin, R., Flanders, W., Vander Griend, D., Mork, E., and Cantrell, P., 2010, Field demonstration of carbon dioxide miscible flooding in the Lansing-Kansas City Formation, Central Kansas: Final Report, Award Number DE-AC26-00BC15124. http://www.kgs.ku.edu/CO2/Reports/Final_Report_March2010.pdf

Dubois, M. K., Williams, E. T., Youle, J. C., and Hedke, D. E., 2015, Potential for CO_2 storage and enhanced oil recovery in four southwest Kansas oil fields, an extended abstract; *in* Modeling CO_2 sequestration in saline aquifer and depleted oil reservoir to evaluate regional CO_2 sequestration potential of Ozark Plateau aquifer system, south-central Kansas, W. L. Watney, J. Rush, and J. Raney, eds.: final report, award number DE-FE0002056, p. IV1–IV19. doi:10.2172/1262248

Gupta, M., Spikes, K., and Hardage, B., 2017, Characterization of naturally fractured Arbuckle Group in the Wellington Field, Kansas, using S-wave amplitude variation with offset: Interpretation, v. 5, no. 1, p. T49–T63.

Hawkes, C. D., Bachu, S., Haug, K., and Thompson, A. W., 2005, Analysis of in-situ stress regime in the Alberta Basin, Canada, for performance assessment of CO_2 geological sequestration sites: Proceedings Fourth Annual Conference on Carbon Capture and Sequestration, p. 2–5.

Holubnyak, Y., Dubois, M., Bidgoli, T., Wreath, D., Watney, L., Stover, S., Newell, D., Fazelalavi, F., Hollenbach, A., Jennings, J., Steincamp, C., Schremmer, J., Jordan, B., Crabtree, B., Christensen, J., McFarlane, D., Doveton, J., Krishnamurthy, K., Byron, M., and Watts, K., 2018, Integrated CCS for Kansas (ICKan) Final Technical Report. doi:10.2172/1491482

Holubnyak, Y., Dubois, M., and Hollenbach, J., 2020, Selecting CO_2 sinks CCUS deployment in South Mid-West Kansas; *in* Gas Injection into Geological Formations and Related

Topics, Y. Wu, J. J. Carroll, M. Hao, and W. Zhu, eds.: Beverly, Massachusetts, Scrivener Publishing, p. 161–183.

Holubnyak, Y., Dubois, M., Hollenbach, J., and Hasiuk, F., 2019, Challenges and opportunities for commercial-scale carbon capture and storage in Kansas: SPE Annual Technical Conference and Exhibition, Society of Petroleum Engineers, p. 1–10.

Holubnyak, Y., Watney, W., Birdie, T., Rush, J., and Fazelalavi, M., 2016, Reservoir modeling of CO_2 injection in Arbuckle saline aquifer at Wellington Field, Sumner County, Kansas: Kansas Geological Survey, Open-File Report 2016-29, 150 p.

Holubnyak, Y., Watney, L., Hollenbach, J., Birdie, T., Fazelalavi, M., Bidgoli, T., Schwab, D., Nolte, A., Tsoflias, G., Victorine, J., Graham, B., Doveton, J., Bruns, J., Blazer, B., and Wreath, D., 2017, Small scale field test demonstrating CO_2 sequestration in Arbuckle saline aquifer and by CO_2-EOR at Wellington Field, Sumner County, Kansas: final report, award number DE-FE00006821. https://www.netl.doe.gov/sites/default/files/2018-02/DE-FE00006821-Final-reportV6.pdf

KGS (Kansas Geological Survey), 2001, Background: The Hugoton Project: an industry-university-government study of the oil & gas resources of southwest Kansas. http://www.kgs.ku.edu/Hugoton/background.html

KGS (Kansas Geological Survey), 2007, Hugoton Asset Management Project (HAMP): Hugoton Geomodel Final Report: Kansas Geological Survey, Open-File Report 2007-6. http://www.kgs.ku.edu//PRS/publication/2007/OFR07_06/index.html

Merriam, D. F., 1963, The geologic history of Kansas: Kansas Geological Survey, Bulletin 162, 317 p.

Metz, B., Davidson, O., and De Coninck, H., eds., 2005, Carbon dioxide capture and storage: Special report of the intergovernmental panel on climate change: New York, Cambridge University Press, 442 p.

Miller, R. D., Raef, A. E., Byrnes, A. P., Lambrecht, J. L., and Harrison, W. E., 2004, 4-D high-resolution seismic reflection monitoring of miscible CO_2 injected into a carbonate reservoir in the Hall-Gurney Field, Russell County, Kansas [Exp. Abs.]: Society of Exploration Geophysicists, p. 2,259–2,262.

Newell, K. D., Watney, W. L., Cheng, W. L., and Brownrigg, R. L., 1989, Stratigraphic and spatial distribution of oil and gas production in Kansas: Kansas Geological Survey, Subsurface Geology Series 9, 86 p.

Ohl, D., and Raef, A., 2014, Rock formation characterization for carbon dioxide geosequestration: 3D seismic amplitude and coherency anomalies, and seismic petrophysical facies classification, Wellington and Anson-Bates Fields, Kansas, USA: Journal of Applied Geophysics, v. 103, p. 221–231.

Rader, K., 1987, Petrographic and subsurface analysis of Pennsylvanian Morrow sandstones of southwestem Kansas: M.S. thesis, University of Colorado, 106 p.

Raef, A. E., Miller, R. D., Byrnes, A. P., and Harrison, W. E., 2005, Rock physics and seismic modeling guided application of 4D-seismic attributes to monitoring enhanced oil recovery CO_2-flood in a thin carbonate reservoir, Hall Gurney Field, Kansas, U.S.A. [Abs.]: Annual conference of the American Association of Petroleum Geologists, June 19–22, 2005, Calgary, Alberta, Canada.

Raef, A. E., Miller, R. D., Franseen, E. K., Byrnes, A. P., Watney, W. L., and Harrison, W. E., 2005, 4D seismic to image a thin carbonate reservoir during a miscible CO_2 flood: Hall-Gurney field, Kansas, USA: The Leading Edge, v. 24, no. 5, p. 521–526.

Schlumberger, 2015, Recommended seismic volume attributes: Schlumberger product sheet poster. https://www.software.slb.com/products/petrel/petrel-geophysics/multitrace-attribute

Schwab, D. R., Bidgoli, T. S., and Taylor, M. H., 2017, Characterizing the potential for injection-induced fault reactivation through subsurface structural mapping and stress field analysis, Wellington Field, Sumner County, Kansas: Journal of Geophysical Research: Solid Earth, v. 122, p. 10,132–10,154. doi:10.1002/2017JB014071

Sullivan, M., Rodosta, T., Mahajan, K., and Damiani, D., 2019, An overview of the Department of Energy's CarbonSAFE Initiative: Moving CCUS toward commercialization: AIChE Journal, e16855.

Watney, W. L., Rush, J., and Raney, J., 2016, Modeling CO_2 sequestration in saline aquifer and depleted oil reservoir to evaluate regional CO_2 sequestration potential of Ozark Plateau aquifer system, south-central Kansas, final report, Award Number: DE-FE0002056. doi:10.2172/1262248

Yielding, G., Freeman, B., and Needham, T., 1997, Quantitative fault seal prediction: AAPG Bulletin, v. 81, p. 897–91.

Youle, J. C., 1991, Sequence stratigraphy of the lower Middle Pennsylvanian in the eastern Hugoton Embayment of southwestern Kansas: Kansas Geological Survey, Open-File Report 91-52, p. 142–172. http://www.kgs.ku.edu/PRS/publication/1991/OFR91_52/Youle/

APPENDIX A

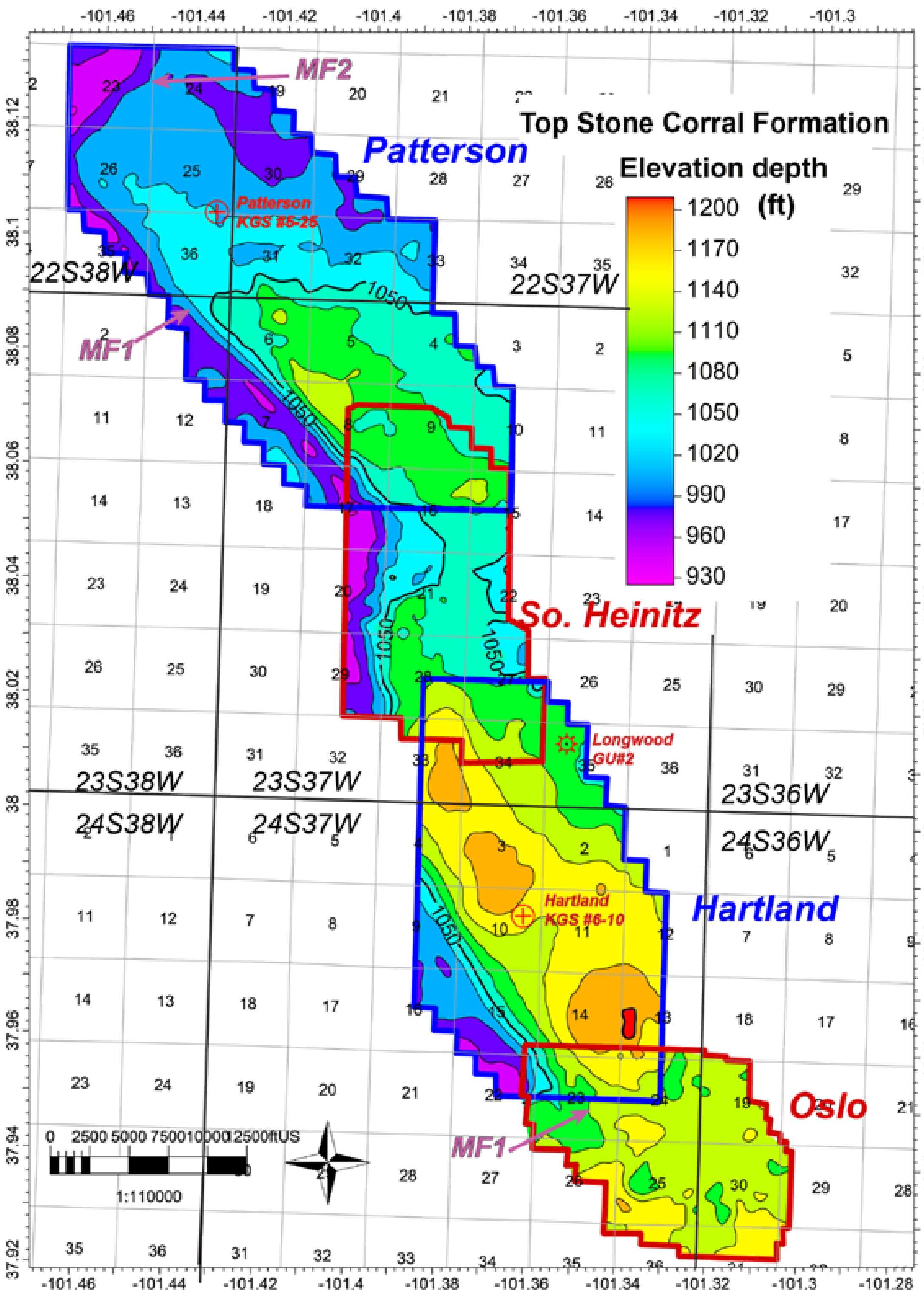

Figure A1. Depth structural contour map of the top of the Stone Corral Formation of the Sumner Group. Contour interval = 30 ft (9 m).

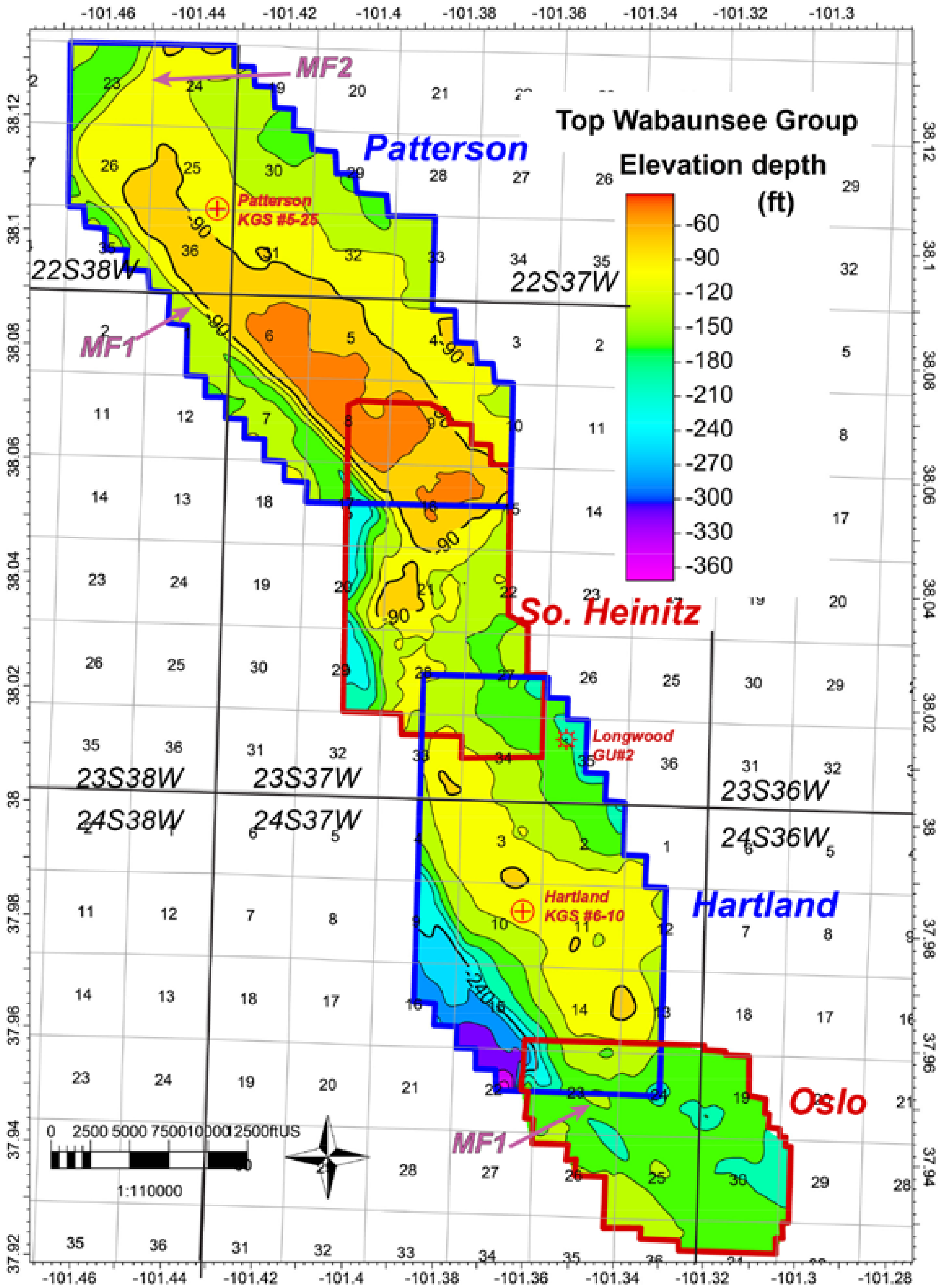

Figure A2. Depth structural contour map of the top of the Wabaunsee Group. Contour interval = 30 ft (9 m).

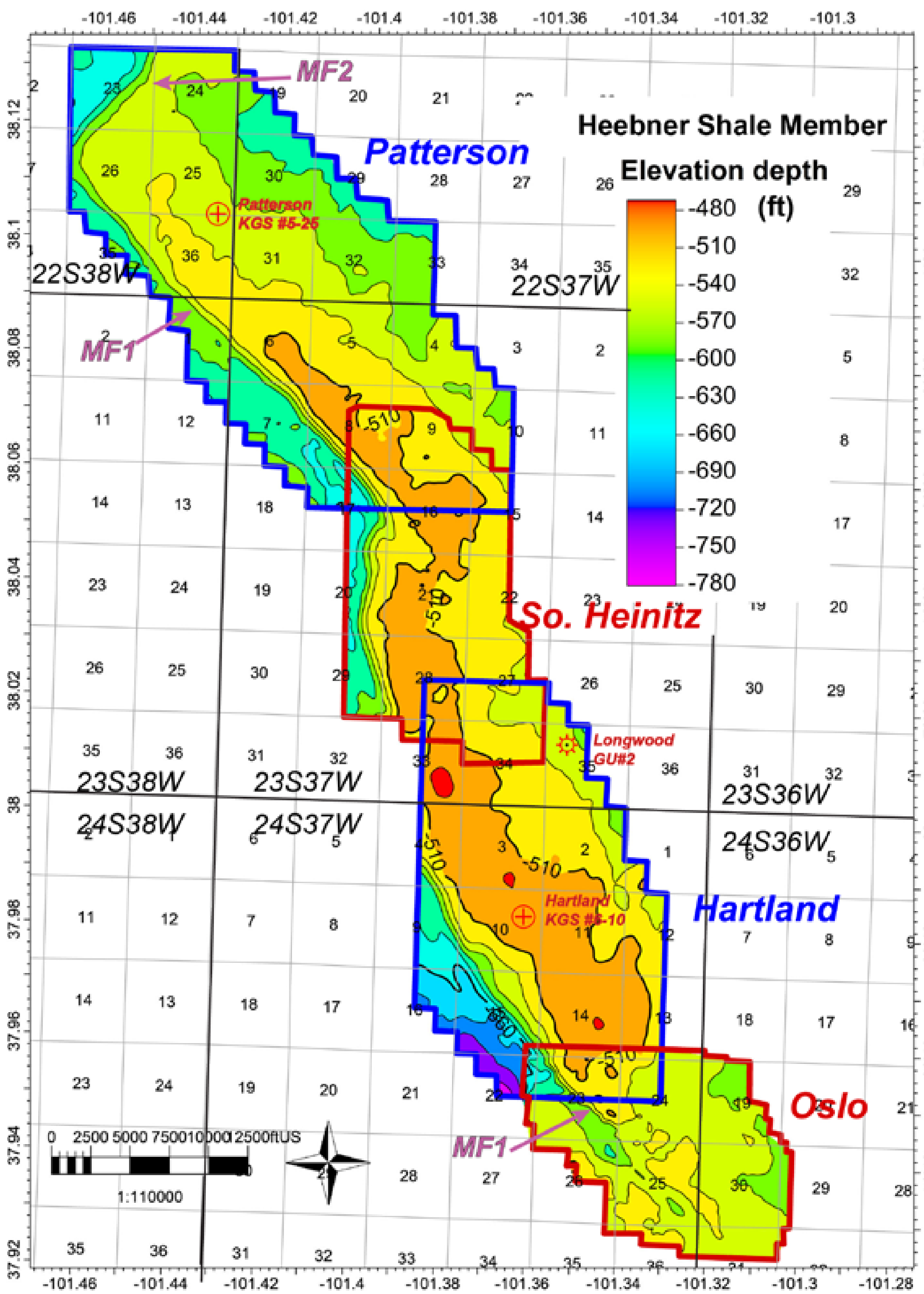

Figure A3. Depth structural contour map of the top of the Heebner Shale Member of the Shawnee Group. Contour interval = 30 ft (9 m).

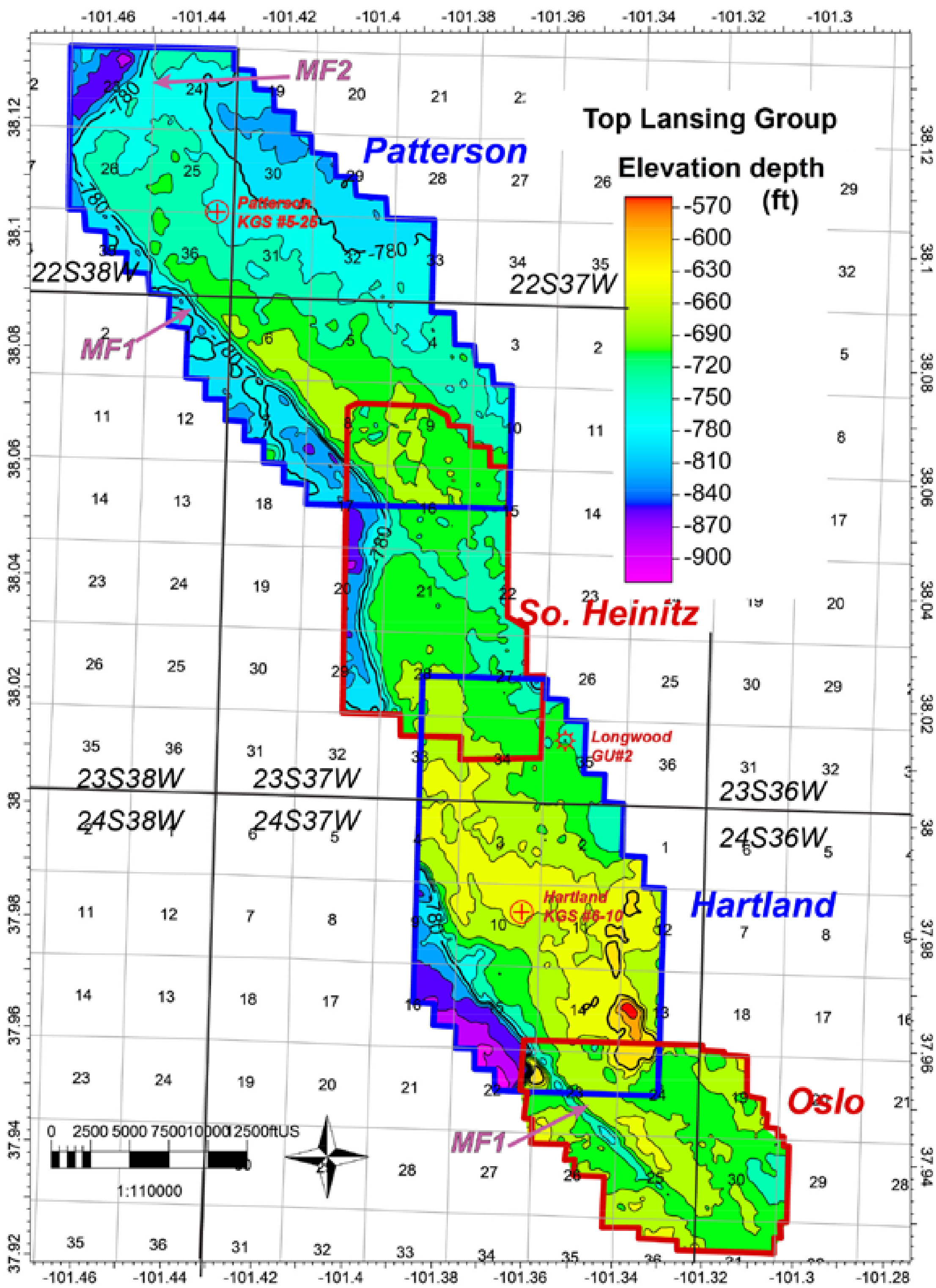

Figure A4. Depth structural contour map of the top of the Lansing Group. Contour interval = 30 ft (9 m).

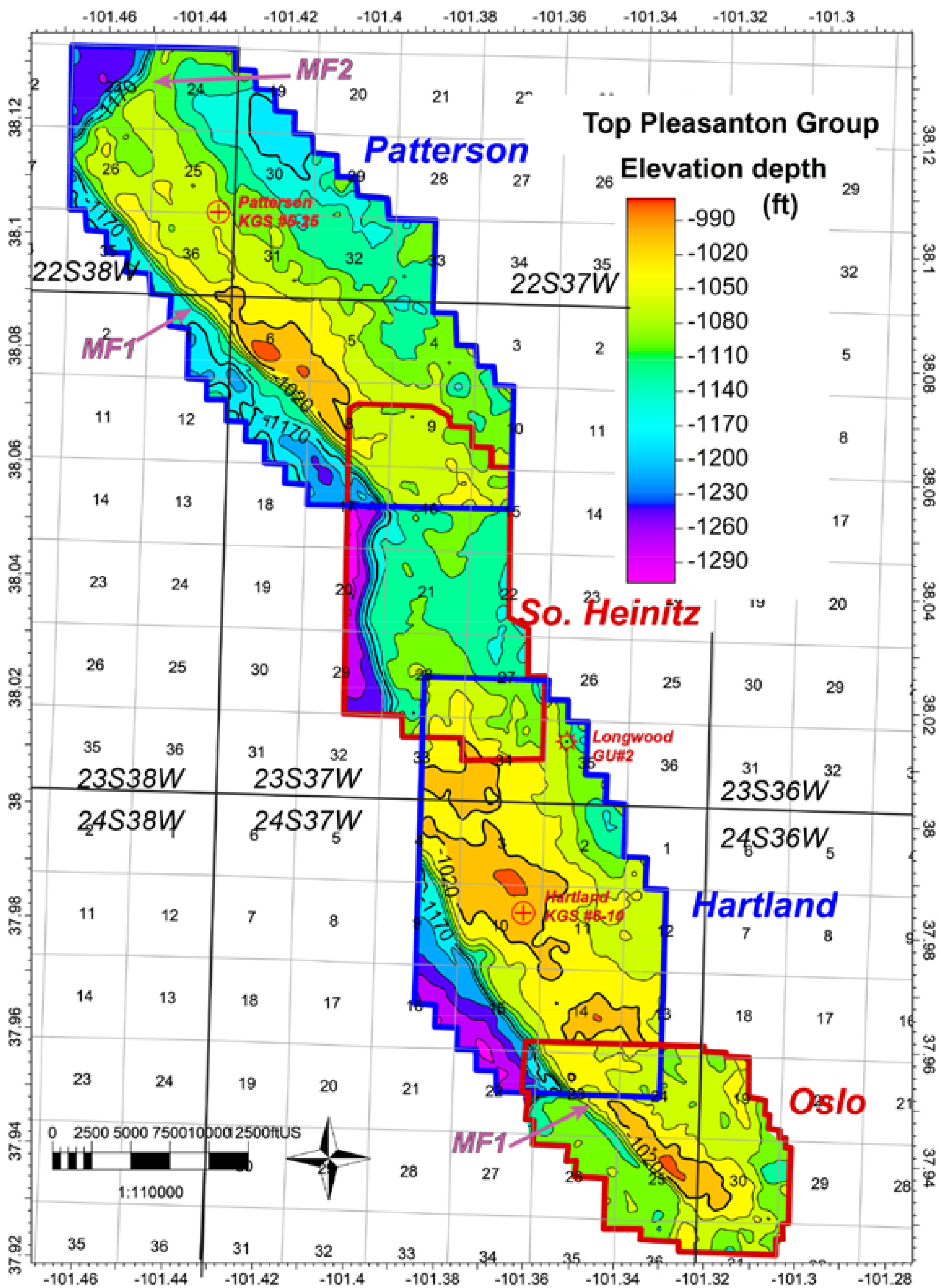

Figure A5. Depth structural contour map of the top of the Pleasanton Group. Contour interval = 30 ft (9 m).

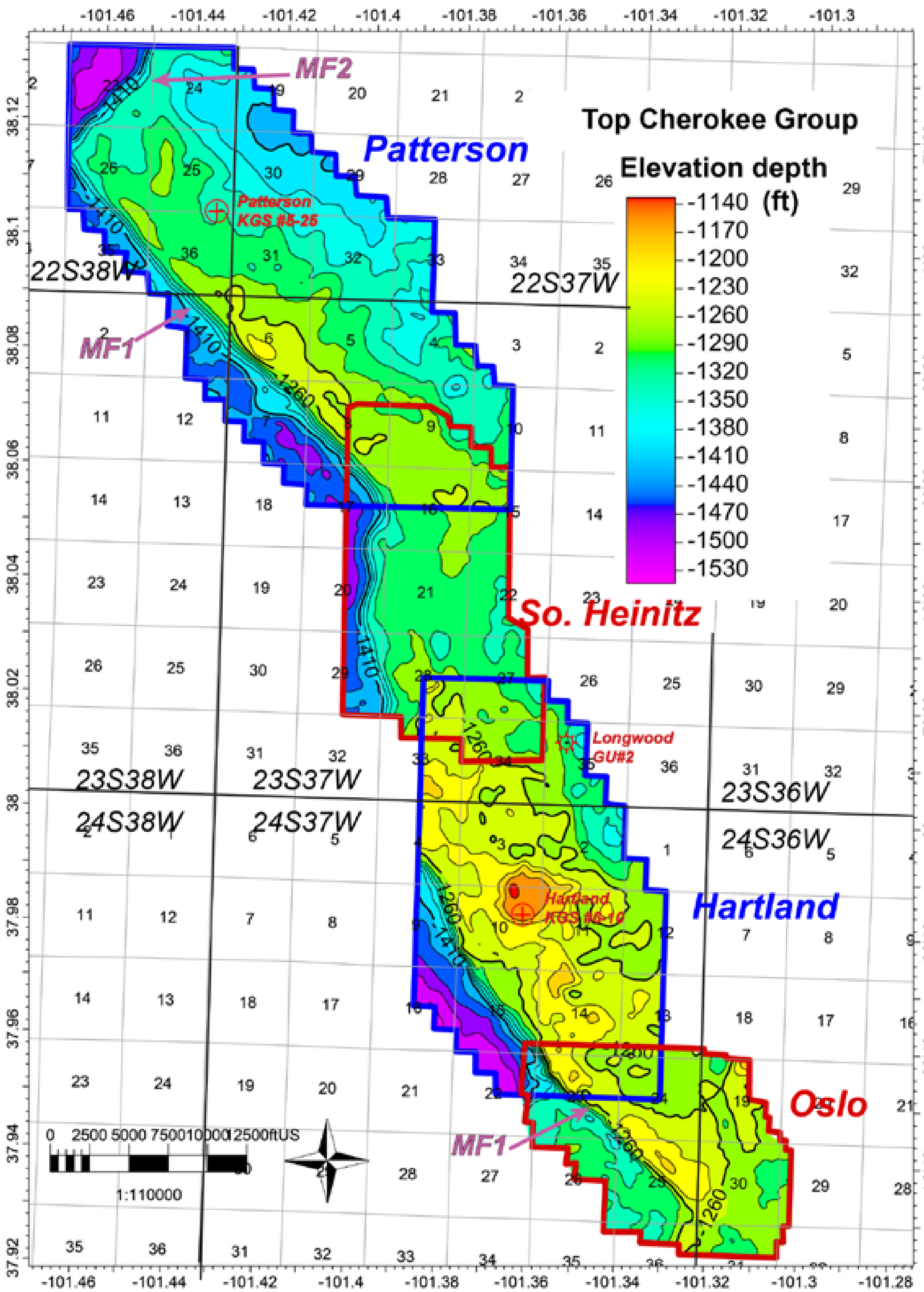

Figure A6. Depth structural contour map of the top of the Cherokee Group. Contour interval = 30 ft (9 m).

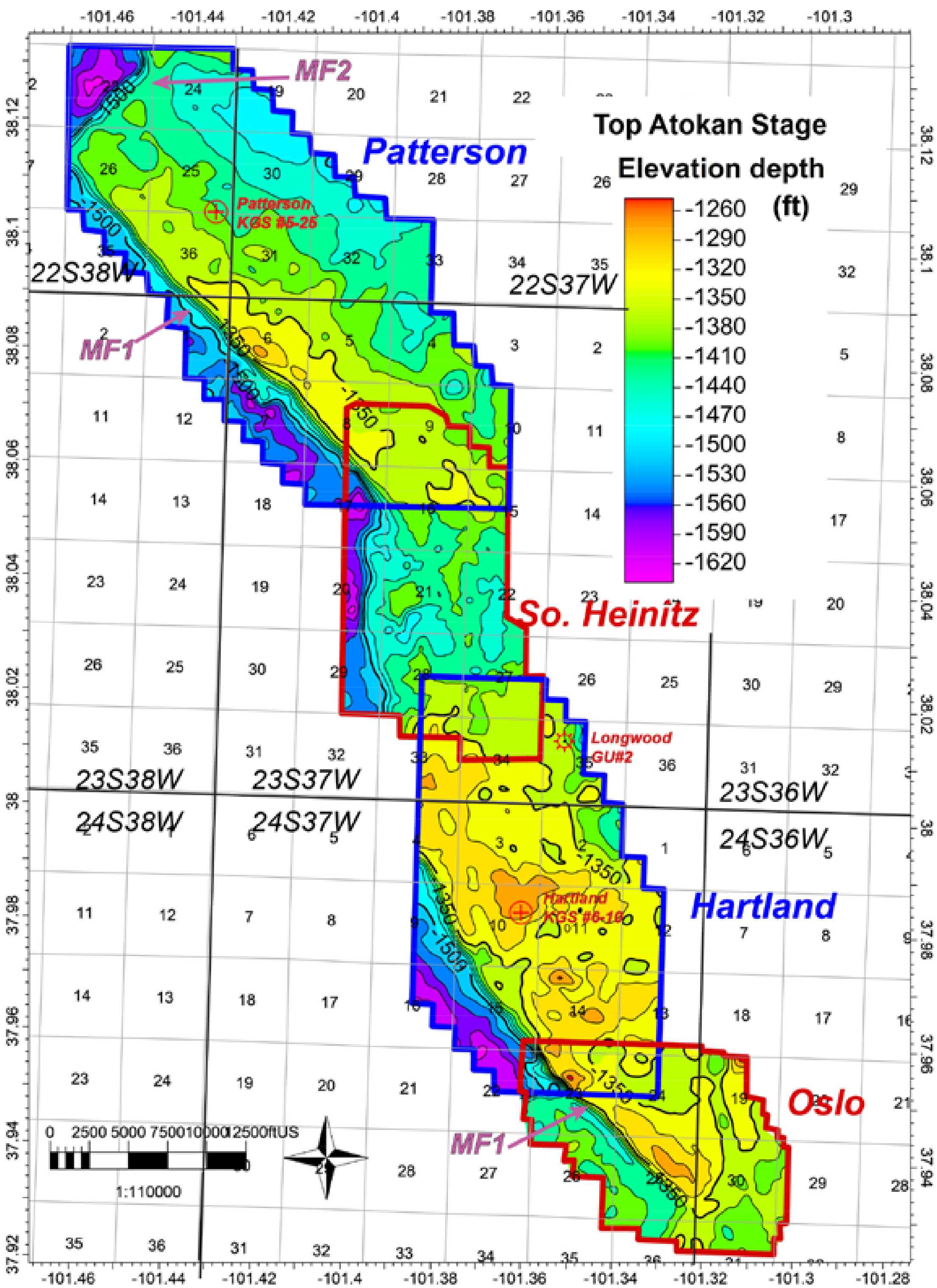

Figure A7. Depth structural contour map of the top of the Atokan Stage. Contour interval = 30 ft (9 m).

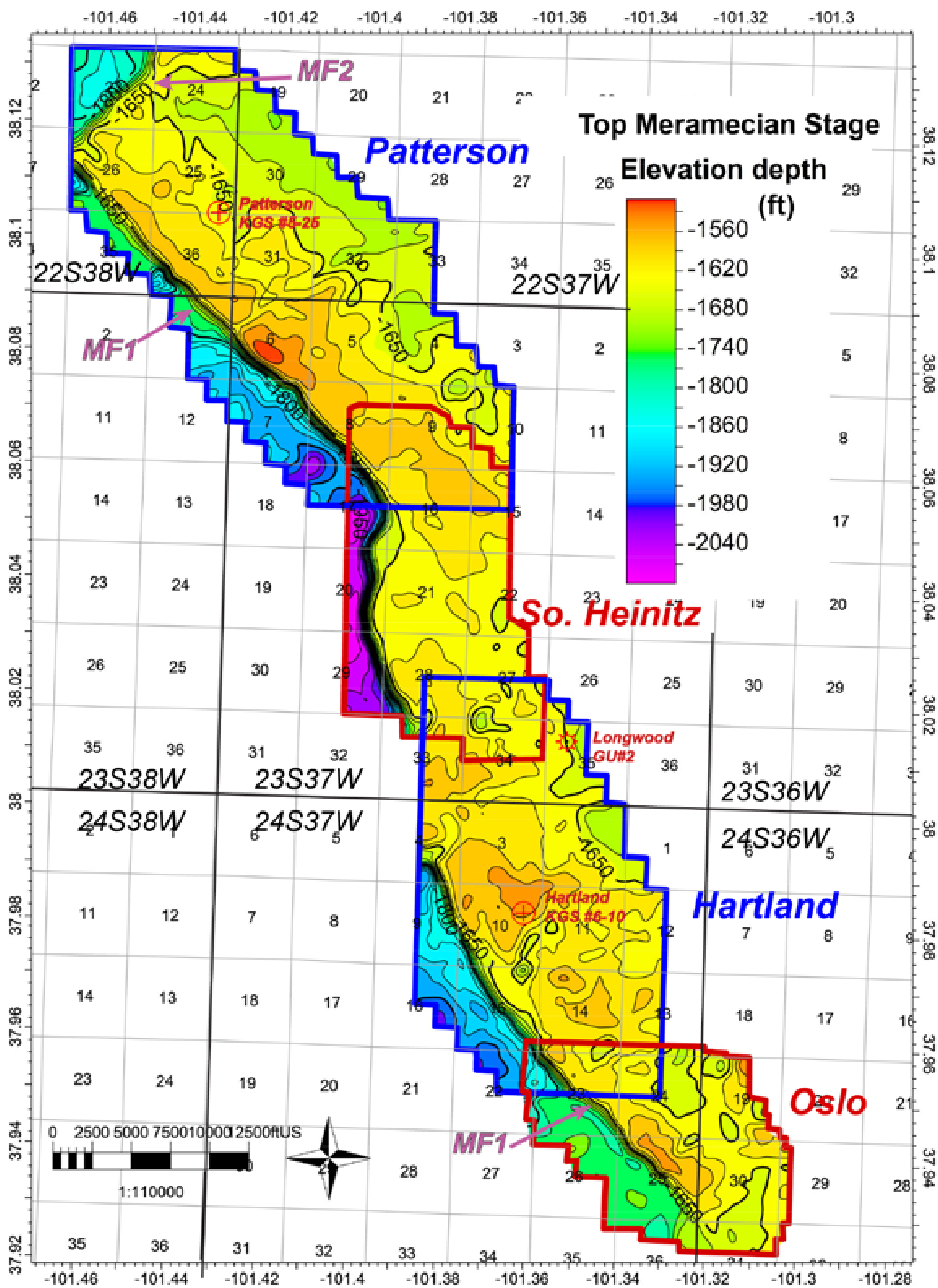

Figure A8. Depth structural contour map of the top of the Meramecian Stage. Contour interval = 30 ft (9 m).

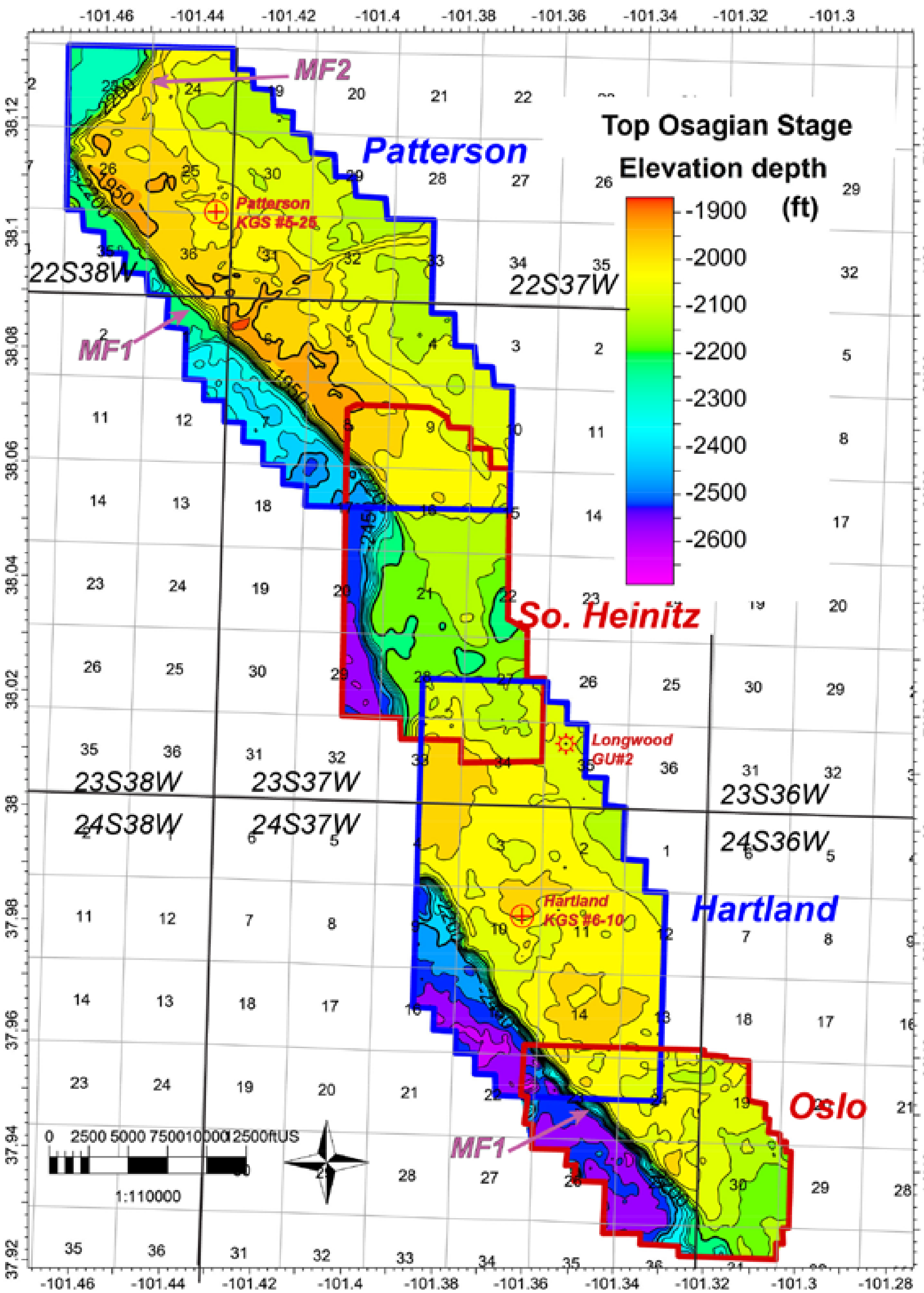

Figure A9. Depth structural contour map of the top of the Osagian Stage. Contour interval = 50 ft (15 m).

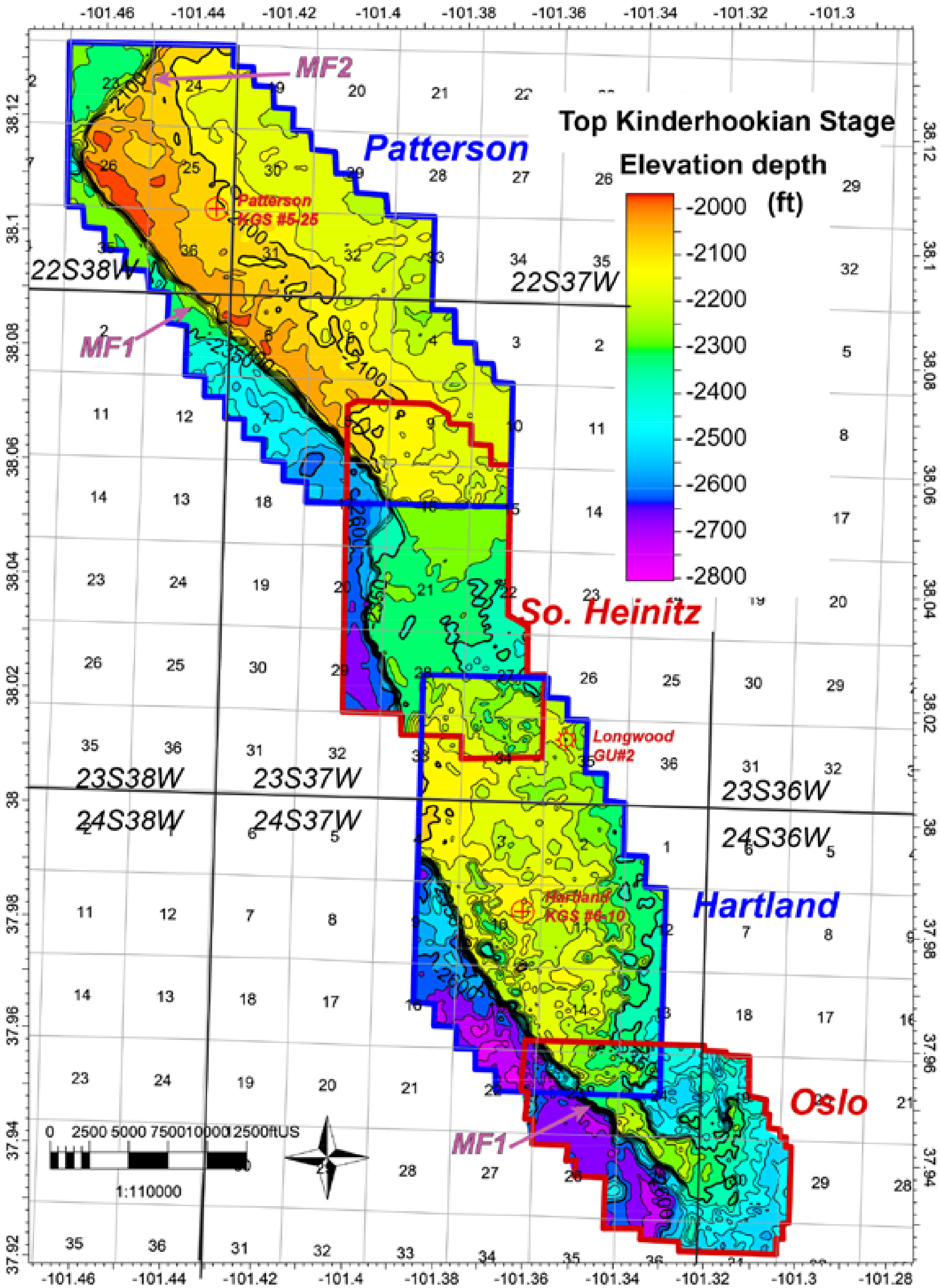

Figure A10. Depth structural contour map of the top of the Kinderhookian Stage. Contour interval = 50 ft (15 m).

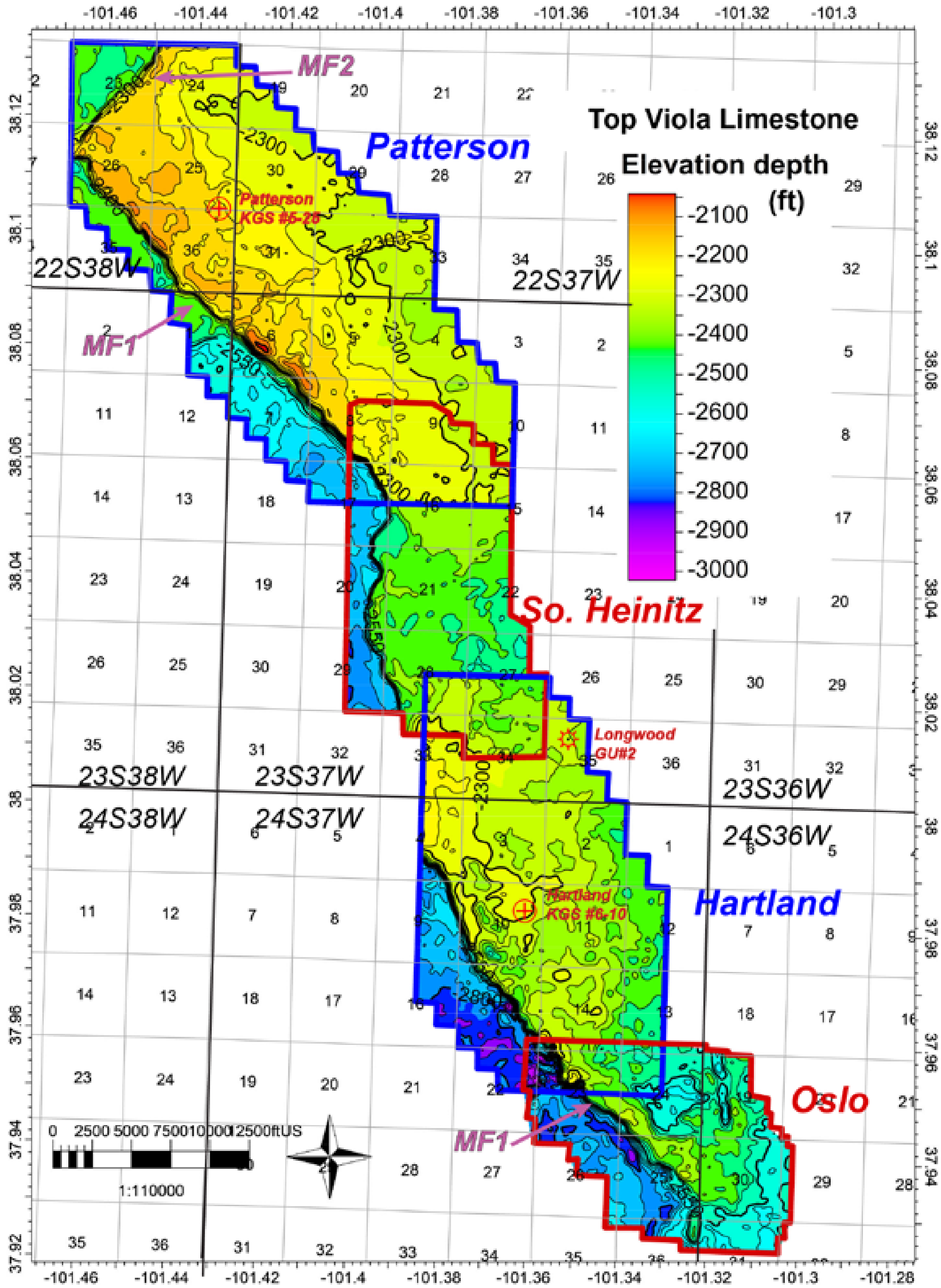

Figure A11. Depth structural contour map of the top of the Viola Limestone. Contour interval = 50 ft (15 m).

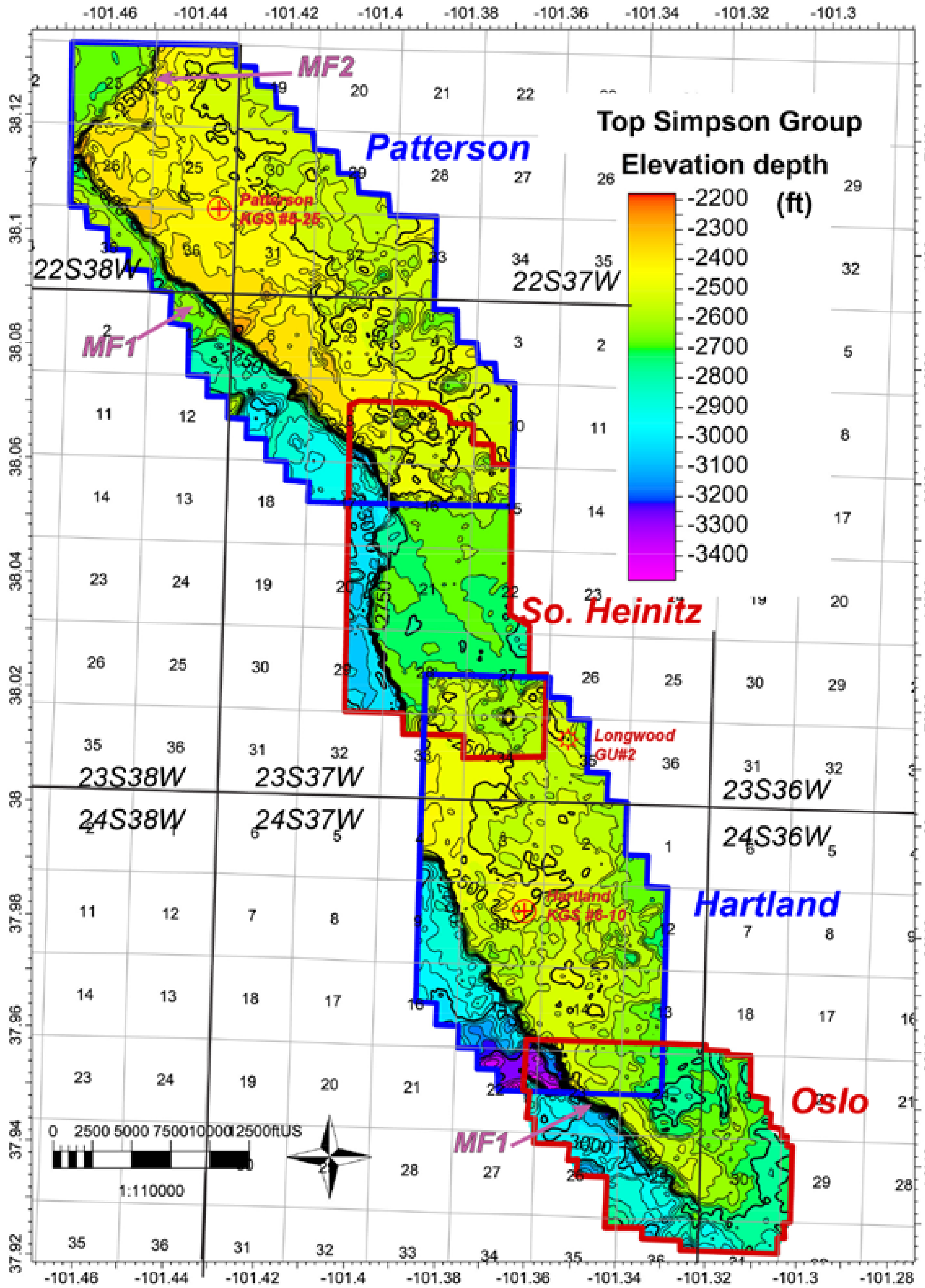

Figure A12. Depth structural contour map of the top of the Simpson Group. Contour interval = 50 ft (15 m).

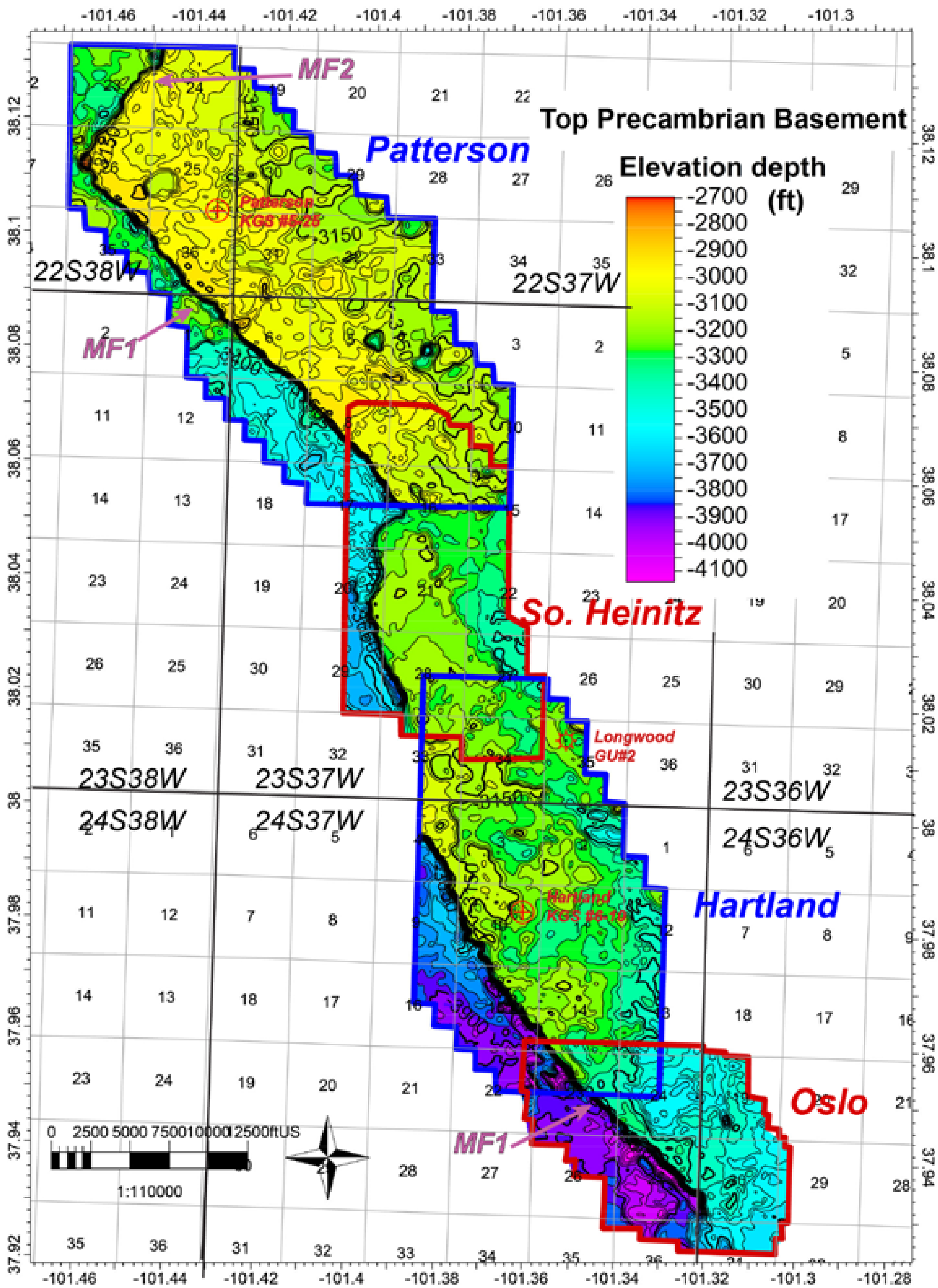

Figure A13. Depth structural contour map of the top of the Precambrian basement. Contour interval = 50 ft (15 m).

APPENDIX B

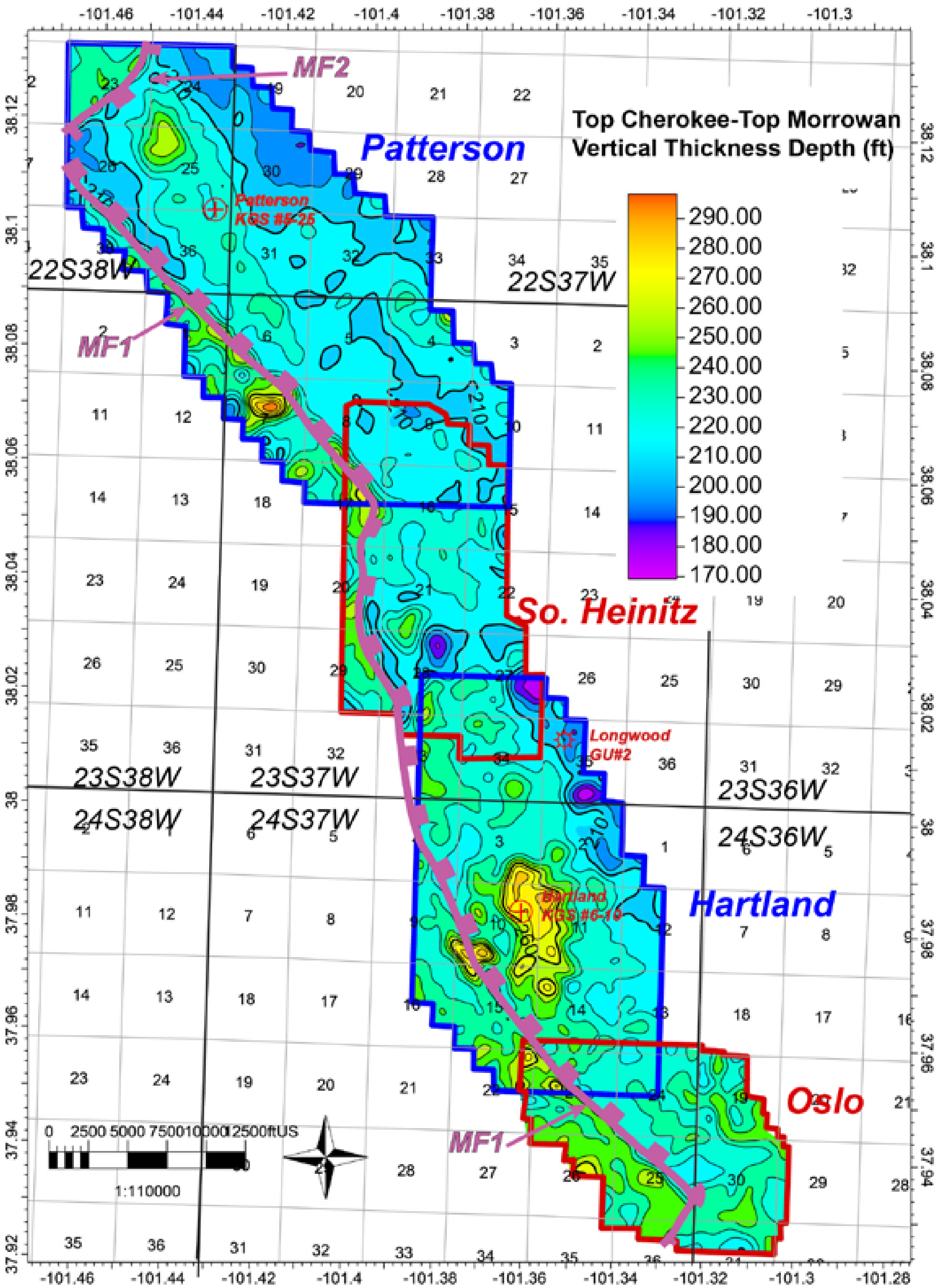

Figure B1. Isopach map of the Cherokee-Morrowan interval. Contour interval = 10 ft (3 m).

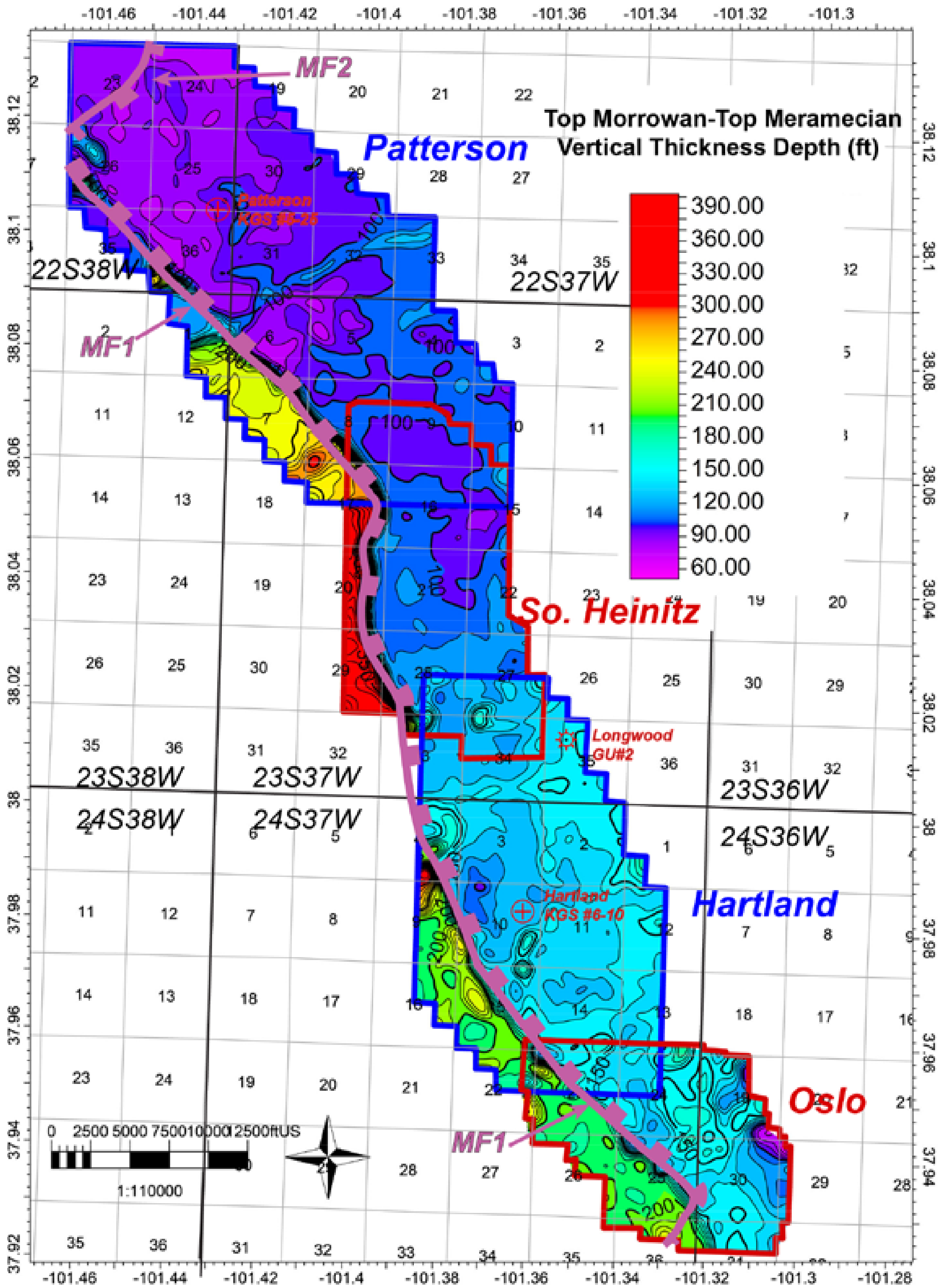

Figure B2. Isopach map of the Morrowan Stage. Contour interval = 10 ft (3 m).

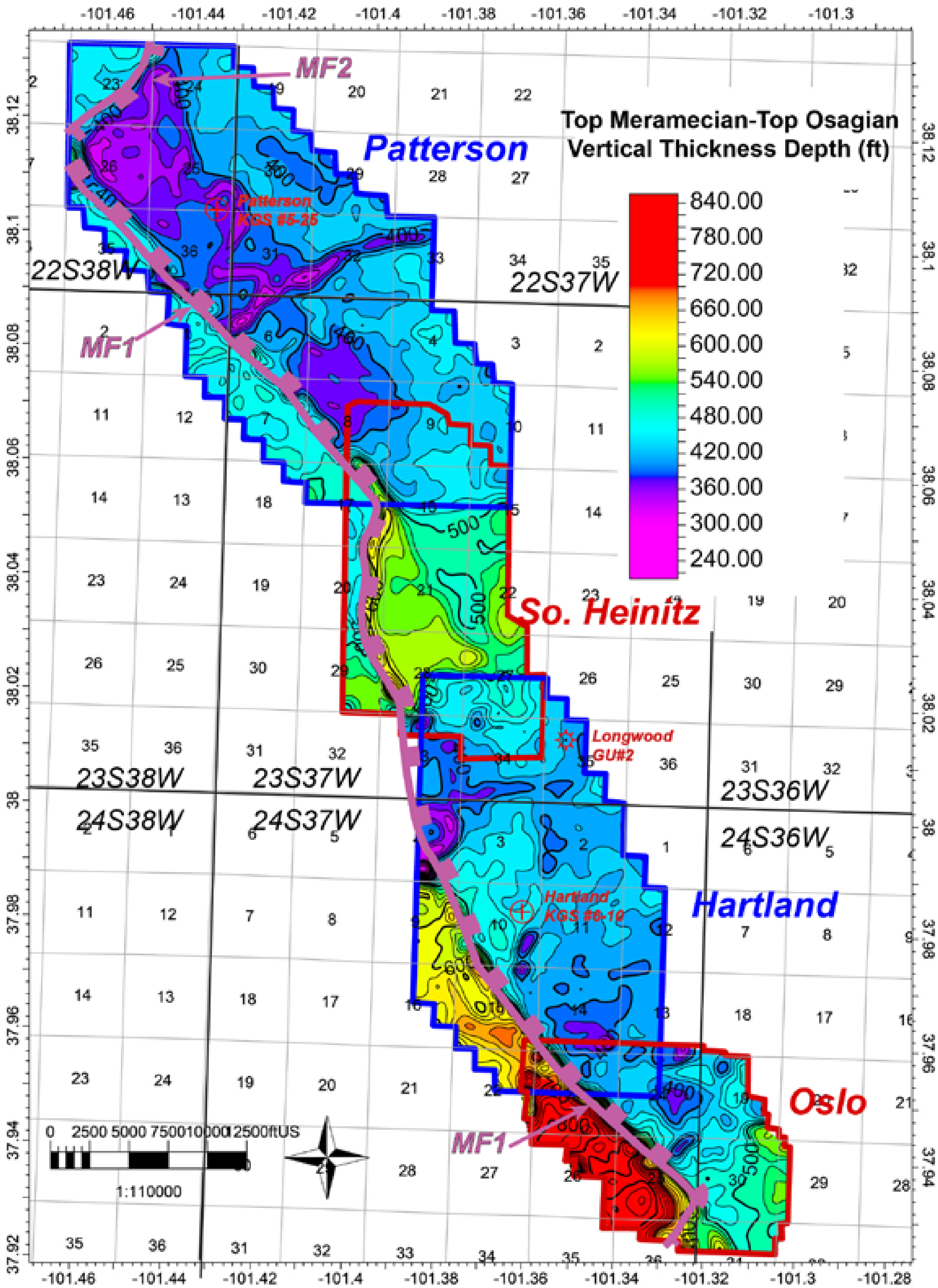

Figure B3. Isopach map of the Meramecian Stage. Contour interval = 20 ft (6 m).

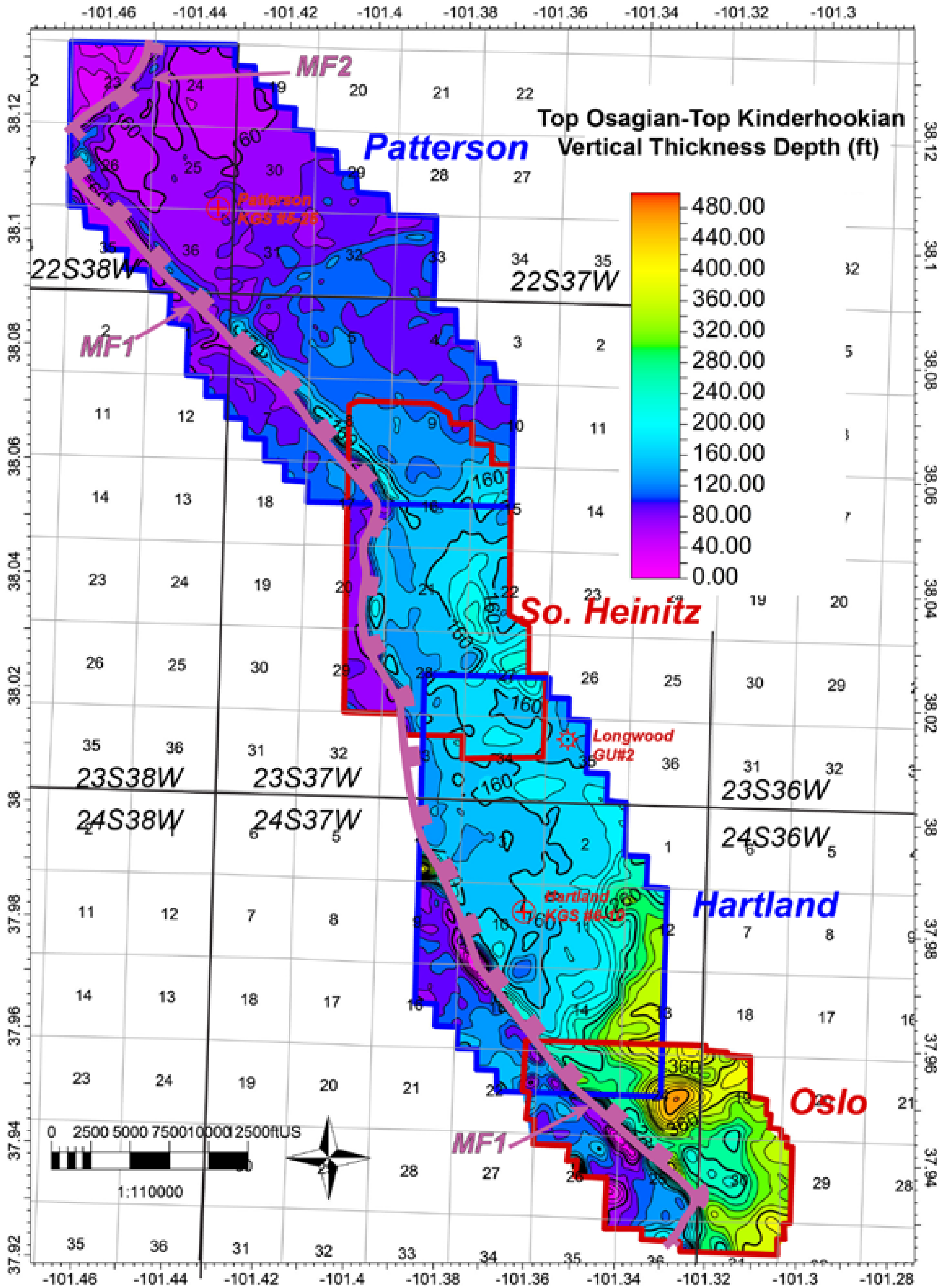

Figure B4. Isopach map of the Osagian Stage. Contour interval = 20 ft (6 m).

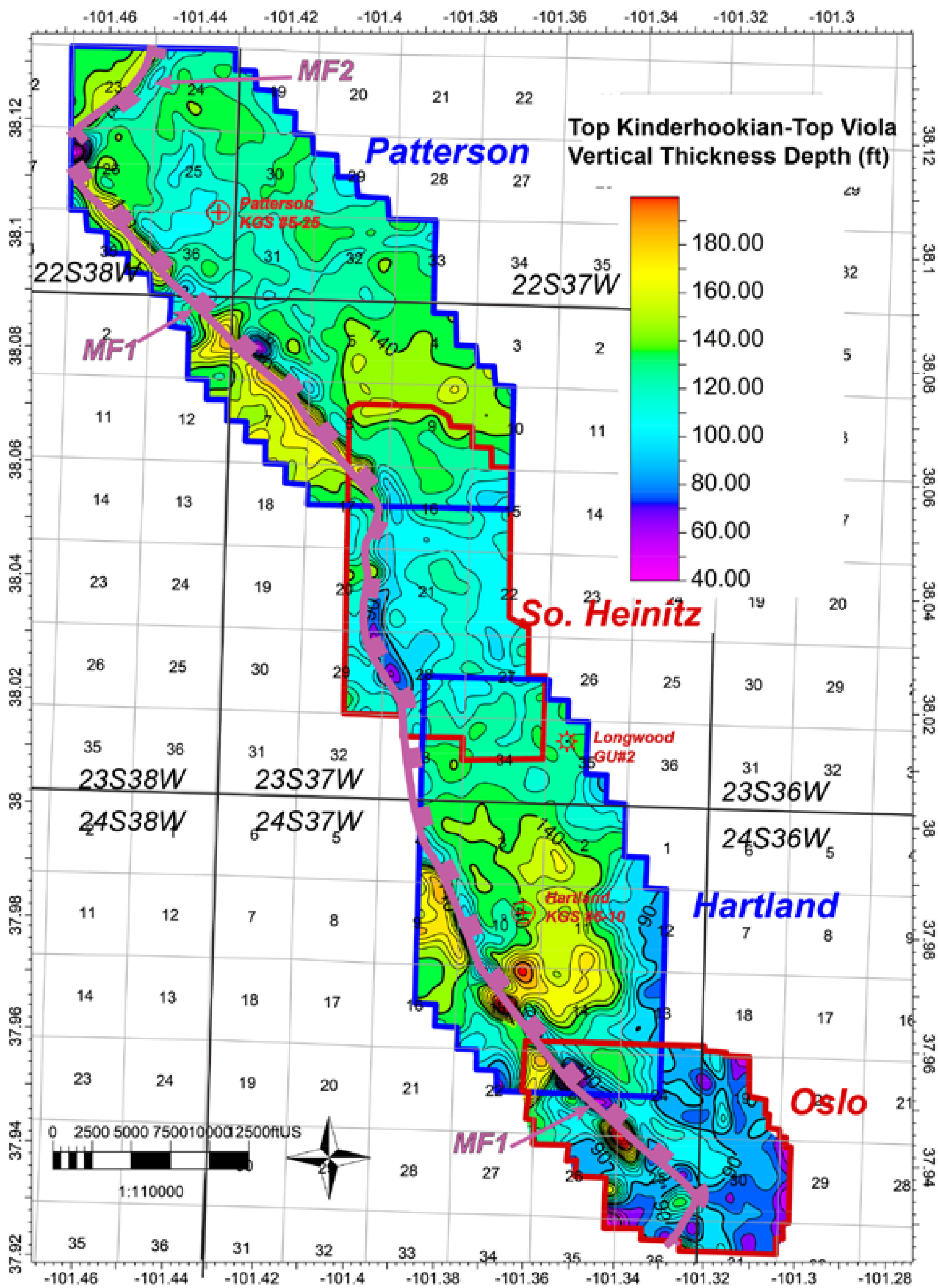

Figure B5. Isopach map of the Kinderhookian Stage. Contour interval = 10 ft (3 m).

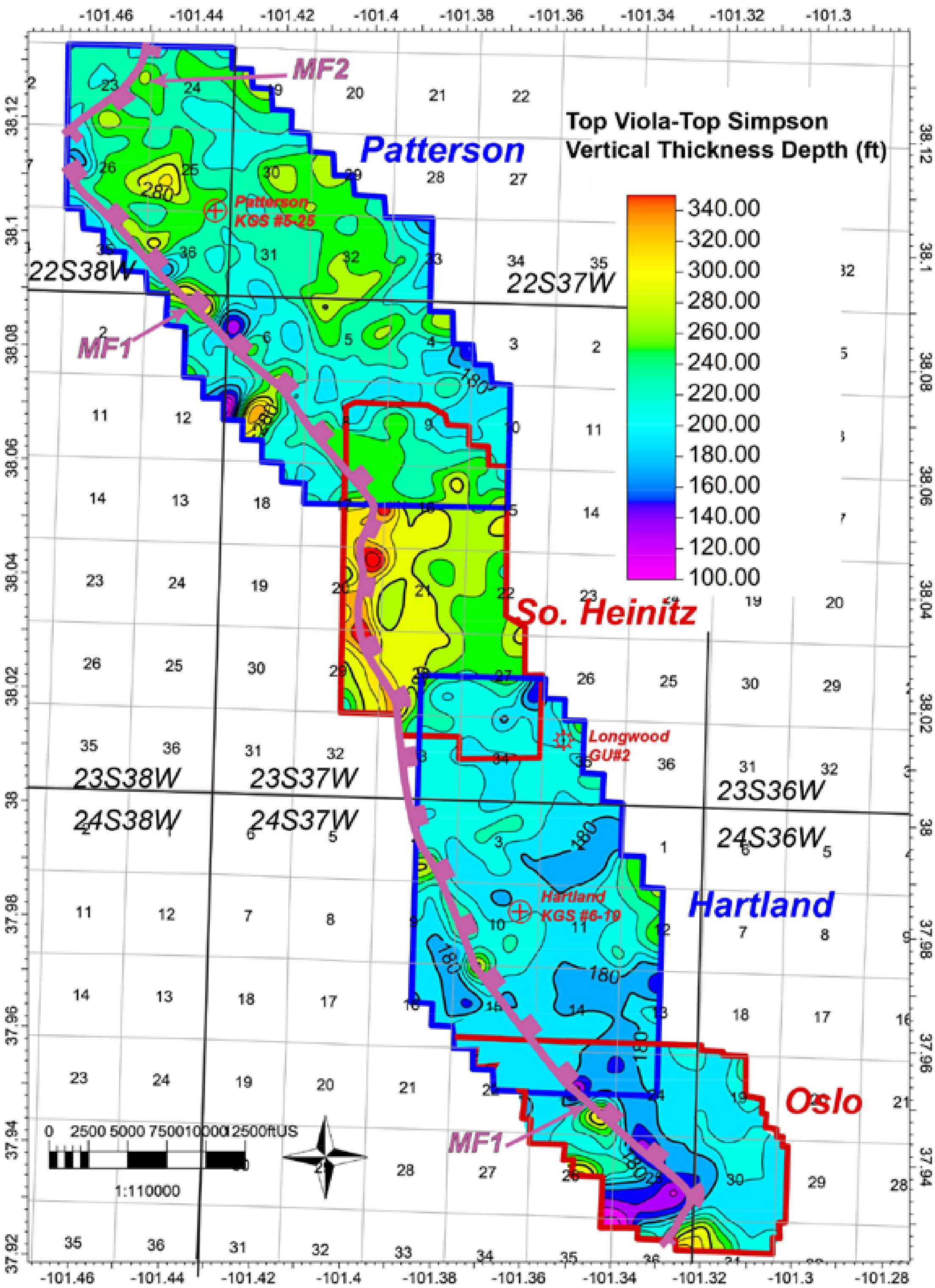

Figure B6. Isopach map of the Viola Limestone. Contour interval = 20 ft (6 m).

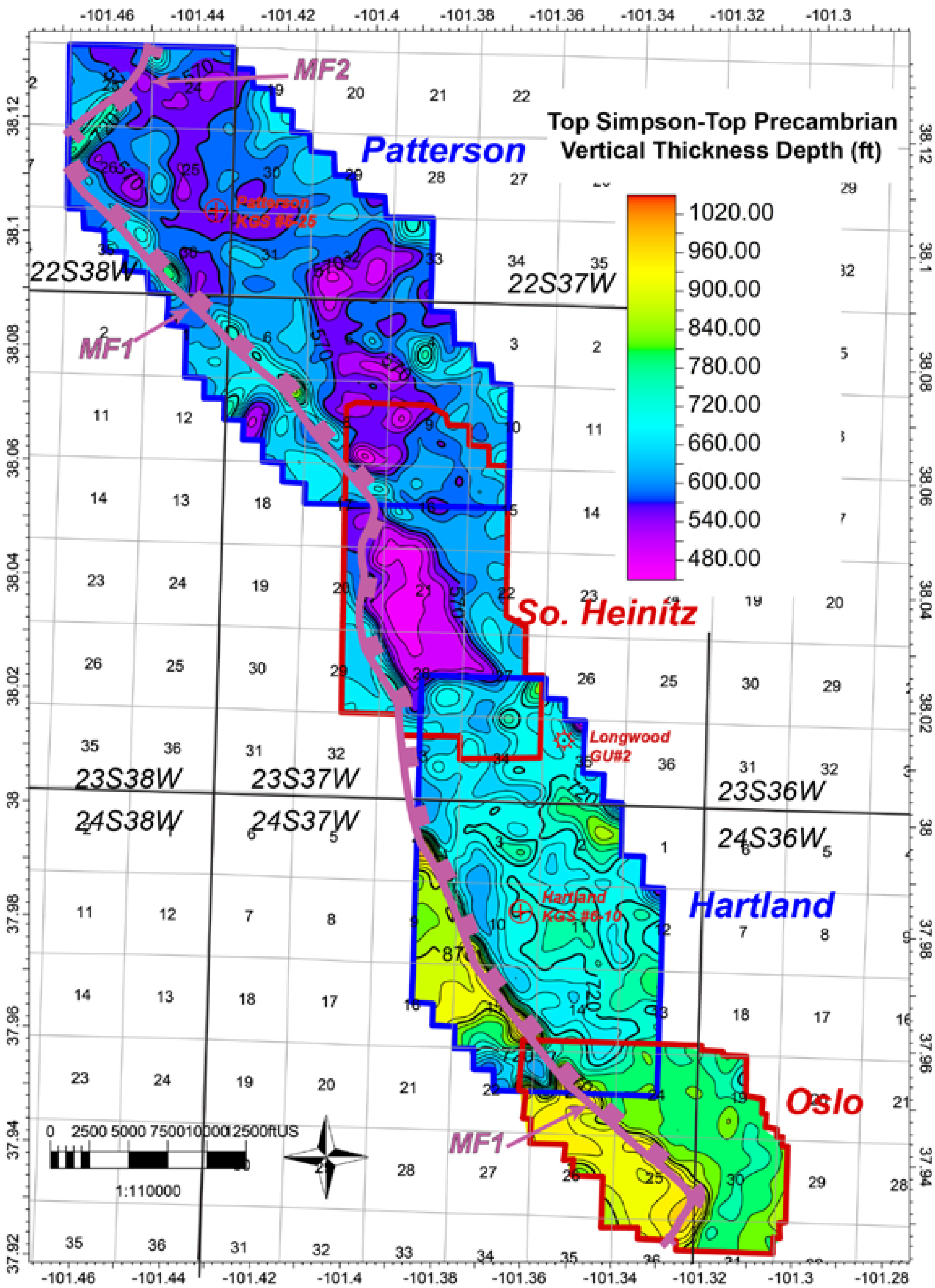

Figure B7. Isopach map of the Simpson-Arbuckle Groups. Contour interval = 30 ft (9 m).

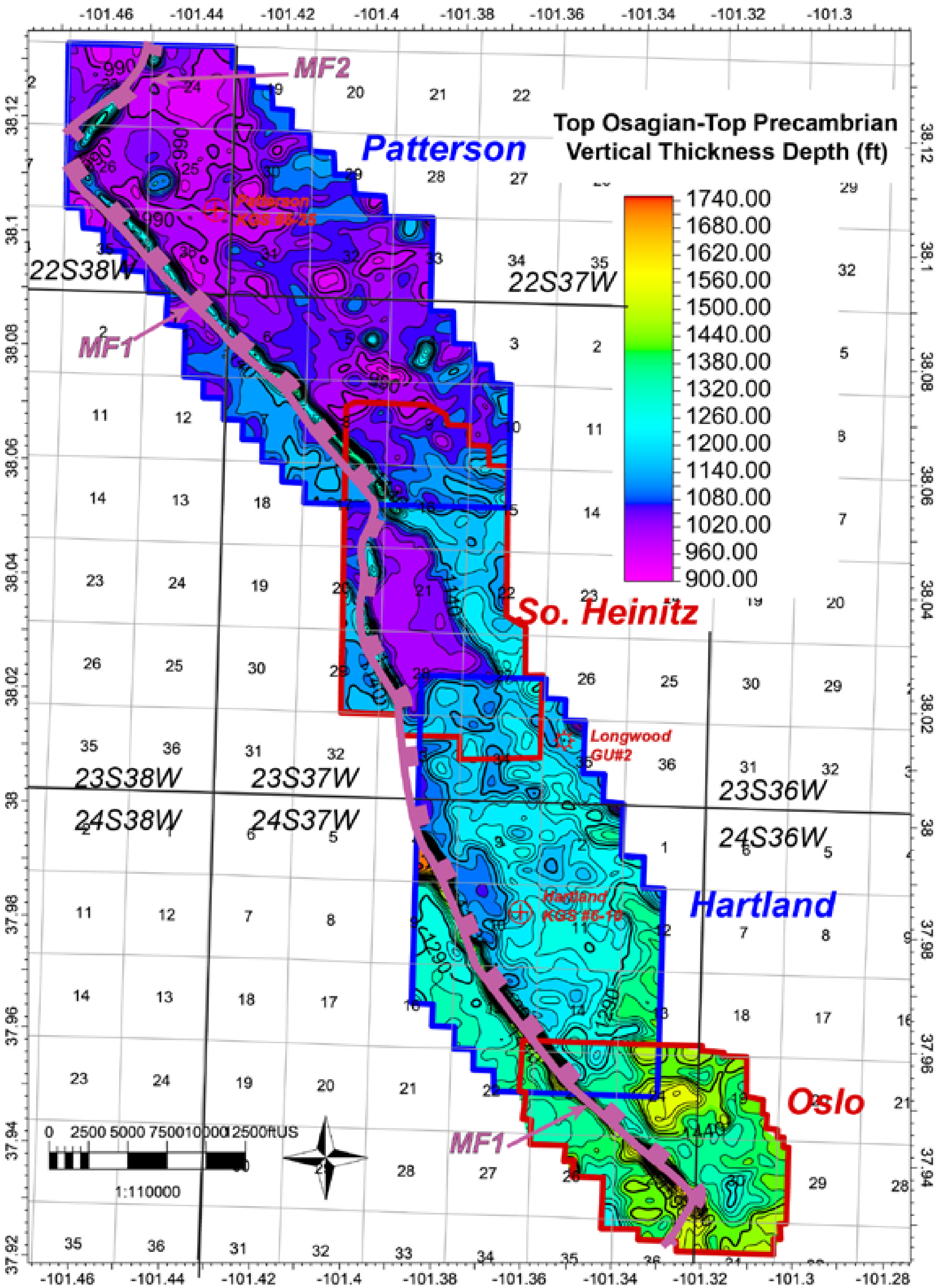

Figure B8. Isopach map of the Osagian Stage-Arbuckle Group showing the accumulated three potential CO_2 storage intervals at the Patterson Site. Contour interval = 30 ft (9 m).

APPENDIX C

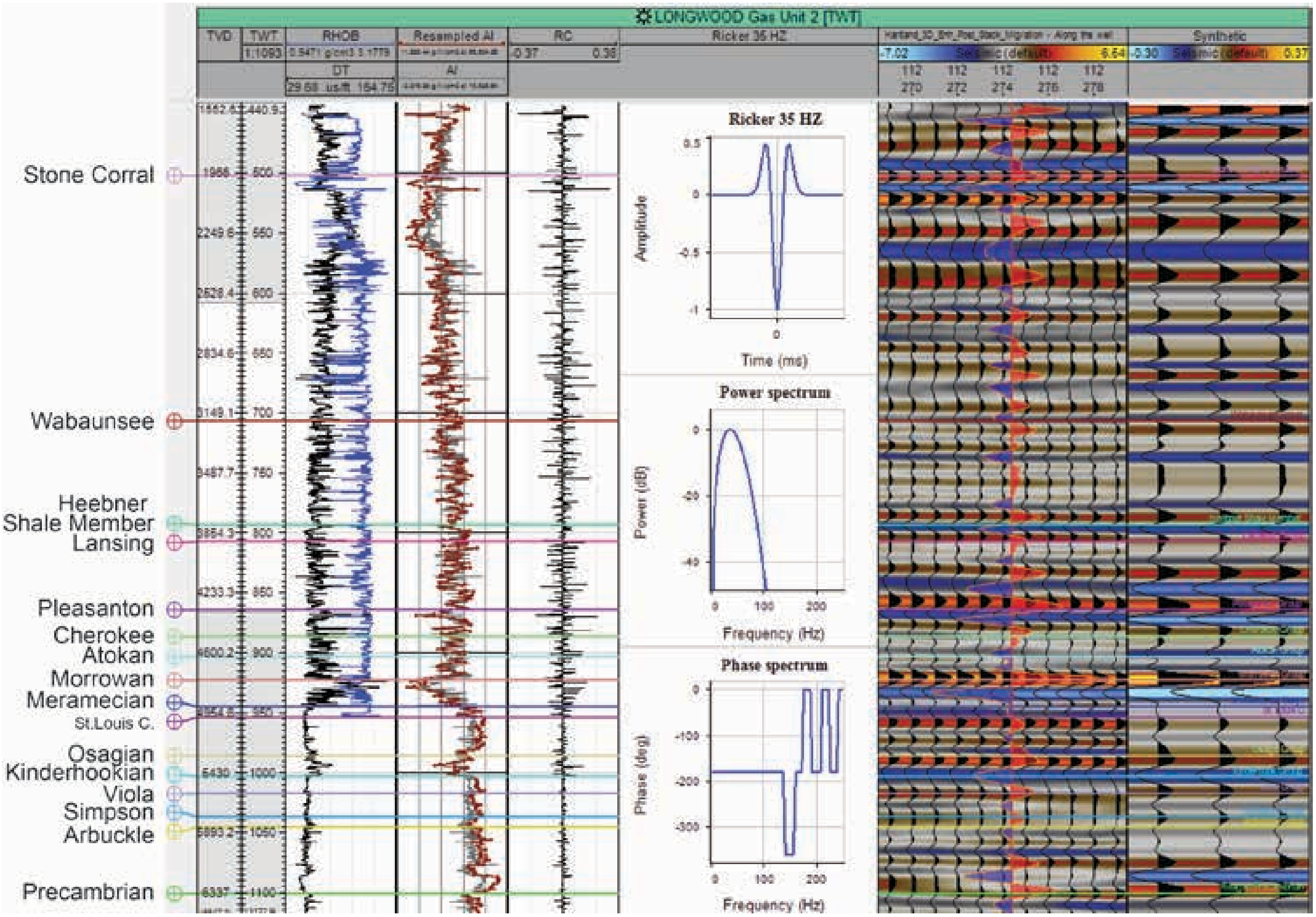

Figure C1. Seismic-to-well tie for the Longwood Gas Unit 2 well.

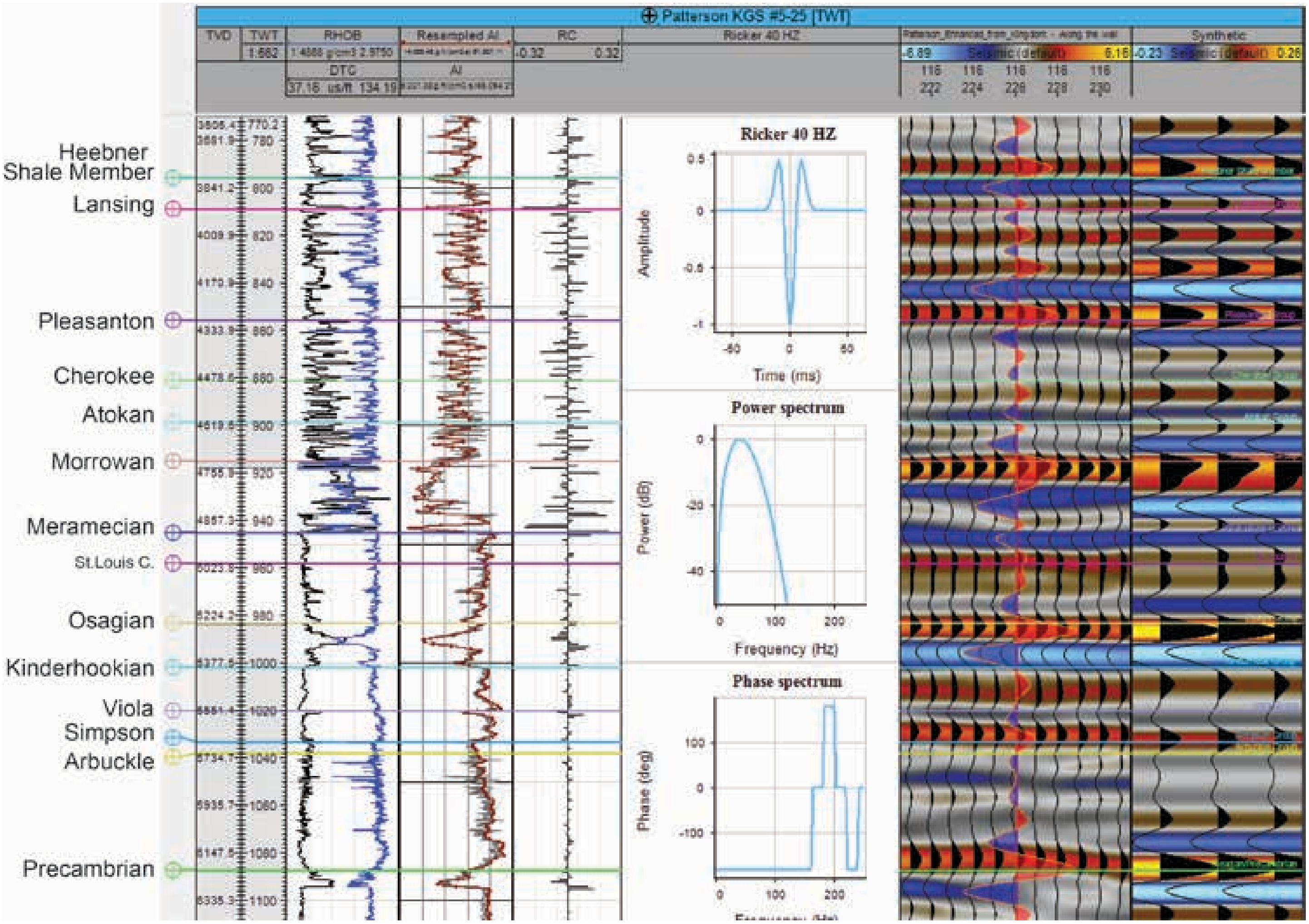

Figure C2. Seismic-to-well tie for the Patterson KGS #5-25 Well.

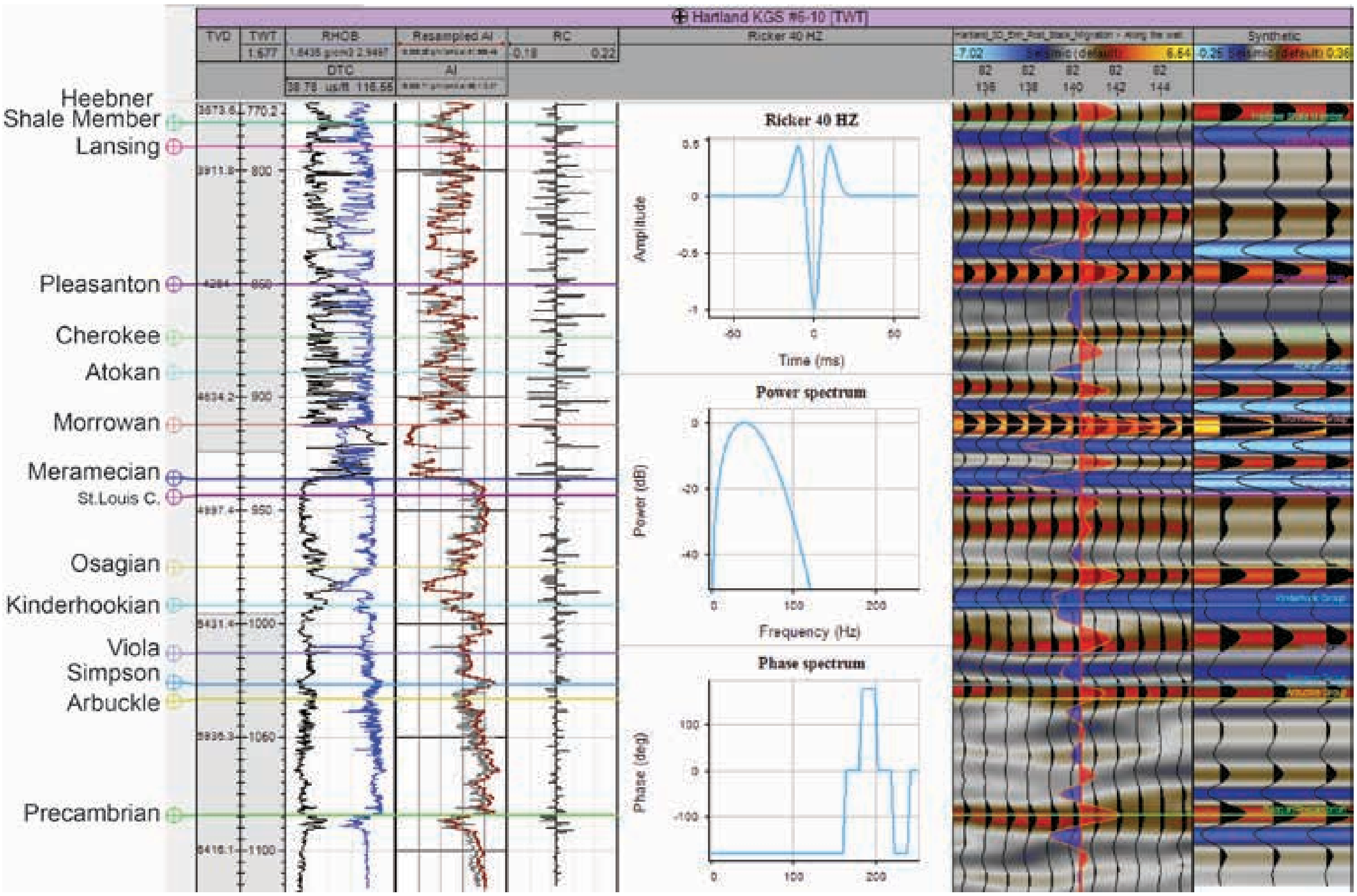

Figure C3. Seismic-to-well tie for the Hartland KGS #6-10 Well.

Midcontinent Geoscience • Volume 1 • November 2020
Tony Layzell – Editor

Section Editor — Jon J. Smith
Technical Editor — Julie Tollefson

Suggested citation: Meng, J., Holubnyak, Y., Hasiuk, F., Hollenbach, J., and Wreath, D., 2020, Geological characterization of the Patterson CO_2 storage site from 3-D seismic data: Midcontinent Geoscience, v. 1, p. 52–90.

Midcontinent Geoscience is an open-access, peer-reviewed journal of the Kansas Geological Survey. The journal publishes original research on a broad array of geoscience topics, with an emphasis on the midcontinent region of the United States, including the Great Plains and Central Lowland provinces.

Submission information: https://journals.ku.edu/mg/about/submissions

Kansas Geological Survey
1930 Constant Avenue
The University of Kansas
Lawrence, KS 66047-3724
785.864.3965

http://www.kgs.ku.edu/

KANSAS GEOLOGICAL SURVEY
The University of Kansas